Erythropoietin signaling in peripheral macrophages is required for systemic β-amyloid clearance

Lu Xu[1,2,3,†], Lei Li[1,†], Cai-Long Pan[1,2], Jing-Jing Song[1], Chen-Yang Zhang[1], Xiang-Hui Wu[1], Fan Hu[4], Xue Liu[1], Zhiren Zhang[5,*] (ID) & Zhi-Yuan Zhang[1,2,3,6,**] (ID)

Abstract

Impaired clearance of beta-amyloid (Aβ) is a primary cause of sporadic Alzheimer's disease (AD). Aβ clearance in the periphery contributes to reducing brain Aβ levels and preventing Alzheimer's disease pathogenesis. We show here that erythropoietin (EPO) increases phagocytic activity, levels of Aβ-degrading enzymes, and Aβ clearance in peripheral macrophages via PPARγ. Erythropoietin is also shown to suppress Aβ-induced inflammatory responses. Deletion of EPO receptor in peripheral macrophages leads to increased peripheral and brain Aβ levels and exacerbates Alzheimer's-associated brain pathologies and behavioral deficits in AD-model mice. Moreover, erythropoietin signaling is impaired in peripheral macrophages of old AD-model mice. Exogenous erythropoietin normalizes impaired EPO signaling and dysregulated functions of peripheral macrophages in old AD-model mice, promotes systemic Aβ clearance, and alleviates disease progression. Erythropoietin treatment may represent a potential therapeutic approach for Alzheimer's disease.

Introduction

Alzheimer's disease is the most common form of dementia and has become a growing global health problem (Lane *et al*, 2018). At present, it is generally accepted that excessive accumulation of neurotoxic Amyloid-β (Aβ) is the initiating factor for the occurrence and development of AD, and disturbances in Aβ clearance are believed to be a primary cause of sporadic AD (Selkoe & Hardy, 2016; Wang *et al*, 2017). Therefore, rather than reducing the Aβ production, increasing Aβ clearance from the brain may be a more promising strategy of AD therapy, particularly for the more common sporadic AD (Zuroff *et al*, 2017). Accumulated data have shown that several pathways, including the blood–brain barrier pathway, lymphatic-related pathway and arachnoid granule pathway, contribute to mediating Aβ effluxes from the brain into the periphery (Cheng *et al*, 2020). Physiological metabolism of Aβ occurs in the brain and periphery, and peripheral Aβ levels can affect Aβ aggregation and clearance in the central nervous system (CNS), because of a physiological balance between brain Aβ and peripheral Aβ, even with intact blood–brain barrier (BBB) (Xiang *et al*, 2015; Wang *et al*, 2017). Recently peripheral and systemic abnormalities in Aβ clearance have been linked to AD pathogenesis and pathological progression (Wang *et al*, 2017), and more recent studies found that Aβ clearance in the periphery contributes substantially to reducing Aβ accumulation in the brain (Cheng *et al*, 2020). Therefore, understanding mechanisms underlying Aβ clearance in the periphery could be important for the development of effective therapies for AD (Cheng *et al*, 2020).

Interestingly, the recent genome-wide association studies (GWASs) of patients with sporadic AD have highlighted the genetic risk factors associated with genetic variation in immunological responses with AD pathogenesis and pathology (Jansen *et al*, 2019; Kunkle *et al*, 2019). Among them, myeloid cells (monocytes/macrophages) have drawn particular attention (Naj *et al*, 2011; Raj *et al*, 2014; Tansey *et al*, 2018), as a variety of sporadic or late-onset AD-risk genes, including *ACE*, *CD2AP*, *APOE*, *BIN1*, *INPP5D*, *CR1*, *ABCA7*, *TREM2*, and *CD33*, have been identified to regulate myeloid cell-mediated Aβ clearance (Zuroff *et al*, 2017). In addition, the enhanced or reduced clearance of Aβ by monocyte system, including monocytes and macrophages, has been found to ameliorate or exacerbate AD related neurological and neuropathological changes, respectively (Guo *et al*, 2019). However, the majority of previous studies have focused on clearance of soluble Aβ by monocytes in circulation or monocyte-derived macrophages

1 School of Basic Medical Sciences, Nanjing Medical University, Nanjing, China
2 Key Laboratory of Antibody Technique of Ministry of Health, Nanjing Medical University, Nanjing, China
3 Department of Neurology, Sir Run Run Hospital, Nanjing Medical University, Nanjing, China
4 State Key Laboratory of Reproductive Medicine, Nanjing Medical University, Nanjing, China
5 Institute of Immunology, Army Medical University, Chongqing, China
6 Key Laboratory of Human Functional Genomics of Jiangsu Province, Nanjing Medical University, Nanjing, China
*Corresponding author. Tel: +86 23 68772229; E-mail: zhangzhiren@tmmu.edu.com
**Corresponding author. Tel: +86 25 86869333; Fax: +86 25 86869331; E-mail: zzy@njmu.edu.cn
†These authors contributed equally to this work

infiltrating into brains, roles played by peripheral tissue macrophages to Aβ clearance remain largely unknown. Nevertheless, Aβ is widely generated by peripheral cells such as platelets, skin fibroblasts, skeletal muscle cells, and osteoblasts (Sun *et al*, 2020), suggesting that peripheral tissue macrophages may contribute to peripheral Aβ clearance. Furthermore, tissue macrophages in liver, spleen and lymph nodes may participate in clearing blood Aβ. Indeed, macrophages of the liver, Kupffer cells have been shown to phagocytosis Aβ in AD patients (Brubaker *et al*, 2017). In addition, monocyte-derived macrophages from AD patients demonstrate ineffective phagocytosis of Aβ compared with the age-matched control subjects (Jairani *et al*, 2019) and dysfunction of peripheral macrophages from aging mice is proved to be involved in cognitive deficits and AD pathogenesis (Minhas *et al*, 2021), indicating that impaired Aβ clearance by peripheral tissue macrophages may contribute to AD pathogenesis. Therefore, understanding roles peripheral tissue macrophages played in systemic Aβ clearance and the underlying mechanisms are of great interest and may provide a new avenue for the treatment of AD.

Notably, Aβ clearance is a dynamic process, allowing host to adapt to their changing microenvironment, particularly Aβ levels. For instance, pretreatment with exogenous Aβ can significantly enhance Aβ clearance by organs like liver and kidney (Tamaki *et al*, 2006; Xiang *et al*, 2015). Aβ also dose-dependently activates serum complement, and complement-opsonized Aβ are eventually captured by erythrocytes (Brubaker *et al*, 2017). In terms of monocytes/macrophages, Aβ can promote itself clearance through activate monocytes/macrophages (Condic *et al*, 2014; Krishnan *et al*, 2020). However, molecules that coordinate expression of Aβ phagocytic genes remain unknown.

Interestingly, Aβ has been shown to induce microglia hypoxia inducible factor-1α (HIF-1α), the oxygen-labile subunit of the HIF complex, which is the master transcription factor for erythropoietin (EPO) (Semenza & Wang, 1992; Herr *et al*, 2009; Baik *et al*, 2019). While EPO is best known to induce hematopoiesis, we and others have shown that EPO suppresses inflammatory gene expression in macrophages and promotes macrophage phagocytosis of apoptotic cells and bacterial (Luo *et al*, 2016a, 2019; Liang *et al*, 2021). However, the involvement of EPO in Aβ clearance remains unknown. In addition, mounting evidences have shown that EPO improves outcomes of AD (Hernandez *et al*, 2017; Rey *et al*, 2019; Sun *et al*, 2019). Nevertheless, while existing researches have mainly focused on possible direct neuroprotective effects of EPO in the brain, EPO is a larger polar macromolecule, even with transporting receptors its penetration of the BBB is limited (Sun *et al*, 2019), indicating that EPO may also function in peripheral to alleviate AD. Here we found that the deficiency of EPO signaling in peripheral macrophages impairs systemic Aβ clearance and deteriorates the progression of AD in mice.

Results

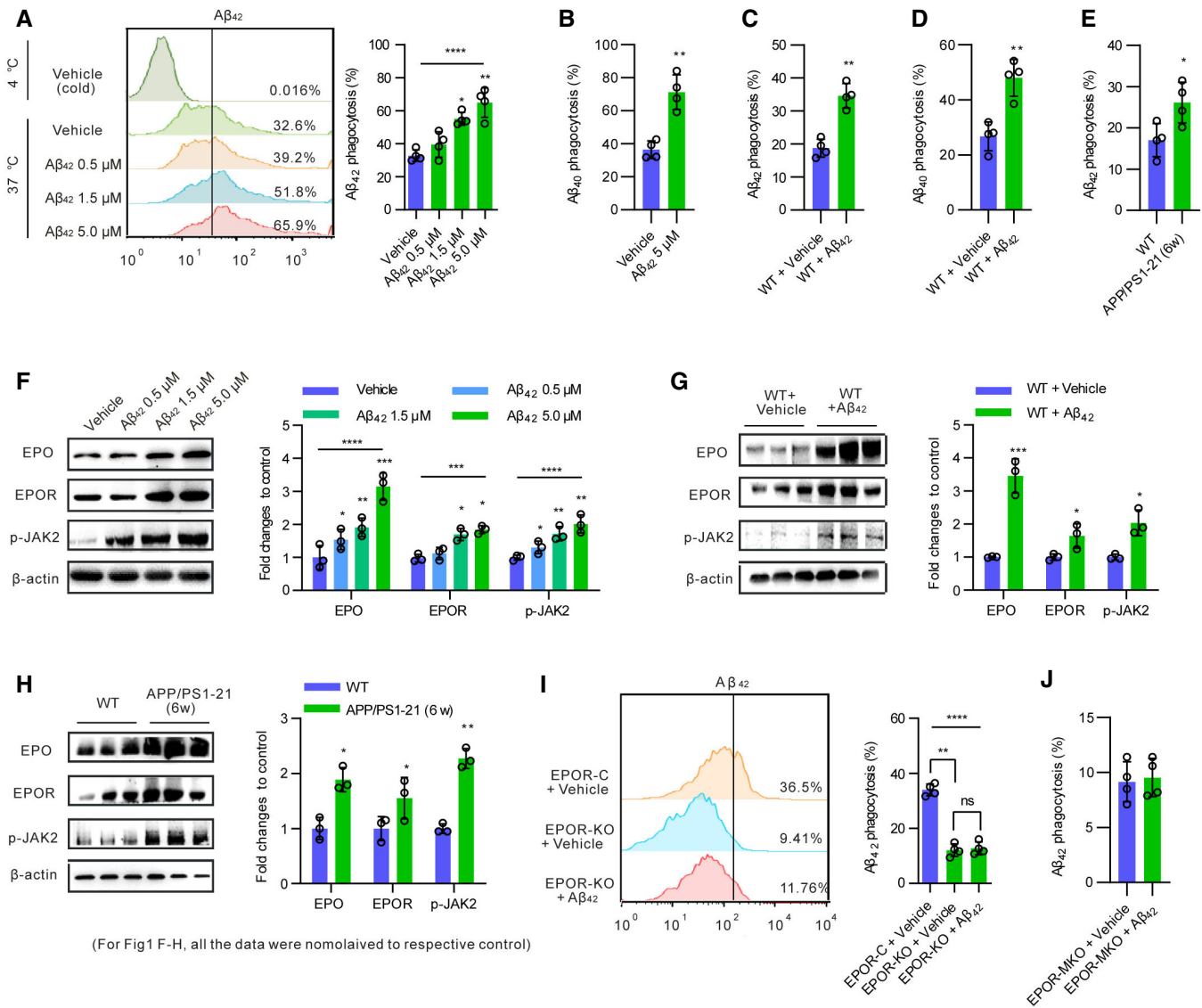## Aβ$_{42}$ promotes itself clearance through EPO signaling in macrophages

To test Aβ uptake by macrophages *in vitro*, peritoneal macrophages (PMs) (Fig EV1A) were incubated with Aβ$_{42}$ or Aβ$_{40}$ for indicated time and Hilyte-Aβ$_{42}$ was then added and incubated at 37°C for 60 min. Incubation at 4°C was used as control, when phagocytosis but not binding to cell surface was suppressed (Luo *et al*, 2016b). Then the PMs were applied for flow cytometry analysis (Fig 1A). Moreover, in some cases, confocal microscopy was used to confirm engulfment (Fig EV1B and C). To further confirm phagocytosis of Aβ, live-cell video microscopy experiment was used. Serial images and video recorded the processes of HiLyte-Aβ phagocytosis of macrophage pre-treated with Aβ$_{42}$ (Fig EV1D and Movie EV1). Given that both endocytosis and phagocytosis has been reported for Aβ$_{42}$ uptake (Heckmann *et al*, 2019), we applied latrunculin A (Park *et al*, 2020) to inhibit phagocytosis and found that Aβ$_{42}$ internalization was prevented (Fig EV1E). Moreover, inhibition of endocytosis with dynasore (Ponath *et al*, 2017) had no effect on Aβ$_{42}$ engulfment (Fig EV1E), indicating that uptake of Aβ$_{42}$ in our model occurs primarily through phagocytosis.

Aβ$_{42}$ pre-stimulation greatly increased macrophage phagocytosis of Aβ$_{42}$ (Figs 1A and EV1B and C) and Aβ$_{40}$ (Fig 1B), but the viability of macrophages was not influenced by Aβ$_{42}$ (Fig EV1F). In stark contrast, Aβ$_{40}$ pre-incubation did not enhance macrophage engulfment (Fig EV1G and H), indicating an Aβ$_{42}$ specific effect. In addition, pre-stimulation with Aβ$_{42}$ also dose-dependently promoted Aβ$_{42}$ phagocytosis by bone marrow-derived macrophages (BMDMs) (Fig EV1I).

Subsequently, we sought to clarify the stimulatory effects of Aβ$_{42}$ on macrophage Aβ phagocytosis *ex vivo*. Twenty-four hours following Aβ$_{42}$ administration, F4/80$^+$ splenic macrophages were purified for Aβ phagocytosis assay by flow cytometry (Fig EV1J). In line with our *in vitro* observations, Aβ$_{42}$ (Fig 1C and D) but not Aβ$_{40}$ (Fig EV1K and L) greatly increased macrophage phagocytosis of Aβ$_{42}$ and Aβ$_{40}$. In addition, significantly higher levels of spleen Aβ$_{42}$ were detected following Aβ$_{42}$ administration (Fig EV1M). Transgenic AD model mice have higher levels of Aβ$_{42}$ (Ashe & Zahs, 2010), therefore we further tested whether the *ex vivo* Aβ$_{42}$ uptake by macrophages in AD model mice was different from that of WT mice. A transgenic mouse model co-expressing the mutated human amyloid precursor protein (APP) and presenilin 1-21 (PS1-21) (APP/PS1-21) was used in our present study. This mouse model is characterized by more aggressive and earlier occurred AD pathology than the well-known APP/PS1 (APPswe, PSEN1dE9) transgenic mouse strain, and that is also accompanied by neuroinflammatory responses and impairments in cognitive, non-cognitive behavioral functions (Radde *et al*, 2006; Gengler *et al*, 2010; Li *et al*, 2020a). Concentrations of Aβ$_{42}$ in spleen of 6-week-old APP/PS1-21 mice were significantly higher (Fig EV1N) and Aβ$_{42}$ phagocytosis by F4/80$^+$ spleen macrophages were also increased correspondingly, compared with that of age and sex-matched WT mice (Fig 1E). Taken together, these data suggest that Aβ$_{42}$ enhances the ability of peripheral macrophage to engulf Aβ$_{42}$ and Aβ$_{40}$.

Aβ$_{42}$ has been shown to induce microglia HIF-1α (Baik *et al*, 2019), which is the master transcription factor for EPO. Our previous investigations showed that EPO promoted macrophage engulfment of apoptotic cells (Luo *et al*, 2016a). While the phagocytosis of Aβ$_{42}$ is different from apoptotic cell phagocytosis by recognition, uptake and degradation (Sole-Domenech *et al*, 2016), they may still share certain common uptake receptors. So, we hypothesized that Aβ$_{42}$ may promote itself uptake through EPO signaling. To test this idea, we first detected whether Aβ$_{42}$ induced the

Figure 1. Aβ$_{42}$ promotes its self-clearance through macrophage EPO signaling.

A, B   Peritoneal macrophages (PMs) were treated with Aβ$_{42}$ (0.5–5 μM) for 12 h, phagocytosis of Aβ$_{42}$ (A) and Aβ$_{40}$ (B) was measured by flow cytometry ($n = 4$). Vehicle (cold) was macrophage treated with Aβ resolution incubated at 4°C. It was used as a negative control to exclude Aβ bound with macrophage from Aβ engulfment. Vehicle was macrophage treated with Aβ resolution incubated at 37°C as control.

C, D   WT mice (8 weeks) were treated with Aβ$_{42}$ (0.2 μmol/kg/day, i.v., twice per day) for 24 h, splenic macrophages were purified for phagocytosis assay of Aβ$_{42}$ (C) and Aβ$_{40}$ (D) ($n = 4$).

E   Splenic macrophages from young APP/PS1-21 mice (6-week-old) were isolated for phagocytosis assay of Aβ$_{42}$ ($n = 4$).

F–H   Macrophages from (A–E) were detected by immunoblotting with the indicated antibodies ($n = 3$).

I   PMs from *Lyz2-Cre$^{+/+}$/Epor$^{loxp/loxp}$* mice (EPOR-MKO) or *Lyz2-Cre$^{+/+}$/Epor$^{+/+}$* mice (EPOR-C) were treated with Aβ$_{42}$ (5 μM) or vehicle for 12 h. Phagocytosis of Aβ$_{42}$ was measured by flow cytometry ($n = 4$).

J   EPOR-MKO mice (8 weeks) were treated with Aβ$_{42}$ (0.2 μmol/kg/day, i.v.) for 24 h, splenic macrophages were used for phagocytosis assay of Aβ$_{42}$ ($n = 4$).

Data information: For multiple groups, one-way ANOVA was used. Unpaired *t*-tests were used for the comparison of two groups. Results are presented as mean ± s.d., *$P < 0.05$, **$P < 0.01$, ***$P < 0.001$ and ****$P < 0.0001$; ns denotes no statistical significance. Aβ, amyloid-β; EPO, erythropoietin. EPOR-KO macrophages were PMs isolated from EPOR-MKO mice.

Source data are available online for this figure.

macrophage EPO signaling. *In vitro*, Aβ$_{42}$ increased the protein amounts of EPO and EPO receptor (EPOR) in PMs in a dose-dependent manner (Fig 1F). Furthermore, the activation of

macrophage EPOR, indicated by JAK2 phosphorylation (p-JAK2), was induced by Aβ$_{42}$ in parallel (Fig 1F). Meanwhile, Aβ$_{42}$ also enhanced the protein amounts of EPO, EPOR and p-JAK2 in F4/80$^+$

spleen macrophages following i.v. given to WT mice (Fig 1G). In addition, these protein levels in macrophages from 6-week-old APP/PS1-21 mice were also higher than that of matched WT mice (Fig 1H). Therefore, $A\beta_{42}$ induced the peripheral macrophage EPO signaling *in vitro* and *in vivo*.

To clarify the contributions of macrophage EPO signaling to $A\beta_{42}$ enhanced itself phagocytosis, we applied PMs from the later mentioned *Lyz2-Cre$^{+/+}$/Epor$^{loxp/loxp}$* (EPOR-MKO) mice in which the EPOR was deleted from macrophages but not from monocytes or neutrophils, as EPOR expresses mainly on macrophages but not the others (Luo *et al*, 2016a). Pre-stimulation with $A\beta_{42}$ did not increase the uptake of $A\beta_{42}$ in EPOR-KO macrophages *in vitro* (Fig 1I), indicating the essential role of EPO signaling. In line with the *in vitro* observations, $A\beta_{42}$ given to *Lyz2-Cre$^{+/+}$/Epor$^{loxp/loxp}$* mice did not increase the $A\beta_{42}$ engulfment by F4/80$^+$ spleen macrophages either (Fig 1J). In addition, our Co-IP assay showed that $A\beta$ did not bind to EPOR directly (Fig EV1O).

In summary, these data indicate that $A\beta_{42}$ increases itself phagocytosis by peripheral macrophages that is mainly mediated by inducing macrophage EPO signaling.

EPO promotes macrophage clearance of $A\beta$ and suppresses $A\beta$-induced inflammatory response

Consequently, we explored whether macrophage EPO signaling was involved in $A\beta$ clearance. Pre-stimulation with recombinant human EPO (rhEPO) for 12 h dose-dependently enhanced $A\beta_{42}$ (Fig 2A) and $A\beta_{40}$ (Fig EV2A) phagocytosis in PMs, without influencing macrophage number and viability (Fig EV2B). In addition, rhEPO also dose-dependently increased $A\beta_{42}$ uptake in BMDMs *in vitro* (Fig EV2C). EPOR-deficient macrophages exhibited a reduction in $A\beta_{42}$ phagocytosis of ~65% *in vitro* and rhEPO could not restore it (Fig 2B). Subsequently, we investigated EPOR-dependent macrophage phagocytosis of $A\beta_{42}$ *ex vivo*. Pre-treatment with rhEPO for 24 h promoted the phagocytosis of $A\beta_{42}$ by F4/80$^+$ splenic macrophages in EPOR-C (*Lyz2-Cre$^{+/+}$/Epor$^{+/+}$*) mice (Fig 2C). The $A\beta_{42}$ engulfment by F4/80$^+$ spleen macrophages was reduced by ~50% in EPOR-MKO mice compared with EPOR-C mice (Fig 2D). Moreover, pre-treatment with rhEPO also enhanced the phagocytosis of $A\beta_{42}$ by F4/80$^+$ splenic macrophages in 5-month-old APP/PS1-21 mice (Fig 2E). In addition, knockout macrophage EPOR expression in APP/PS1-21 mice (*APP/PS1-21/Lyz2-Cre$^{+/+}$/Epor$^{loxp/loxp}$*) decreased the engulfment of $A\beta_{42}$ by F4/80$^+$ splenic macrophages compared with APP/PS1-21 mice (*APP/PS1-21/Lyz2-Cre$^{+/+}$/Epor$^{+/+}$*) (Fig 2F). Together, these data suggest that macrophage EPO signaling promotes $A\beta$ phagocytosis.

Following engulfment, $A\beta$ is degraded inside cells by enzymes, such as insulin degrading enzyme (IDE) and neprilysin (NEP) (Zuroff *et al*, 2017), so we detected EPO effects on their expression. While rhEPO alone did not increase their levels, rhEPO further enhanced $A\beta_{42}$-induced up-expression of IDE and NEP in PMs *in vitro*, but the deficiency of EPOR abolished these effects (Fig EV2D). Similarly, EPO also induced their expression in F4/80$^+$ splenic macrophages in EPOR-C mice (Fig EV2E) and APP/PS1-21 mice (Fig EV2F) *in vivo*, which was abolished by depletion of EPOR in macrophages.

$A\beta_{42}$ can induce inflammatory cytokines in macrophages (Xu *et al*, 2021), so we further measured contributions of EPOR

signaling to that. rhEPO dose-dependently decreased levels of inflammatory mediators TNF-α, IL-1β, IFN-γ, IL-6 and iNOS but increased levels of anti-inflammatory mediators Arg-1 and IL-10 (Fig 2G) in PMs *in vitro* in the existence of $A\beta_{42}$. Levels of IL-1β, IL-6, iNOS and IL-10 in supernatants showed the same pattern (Fig EV2G). EPOR deficiency abolished these effects even with rhEPO treatment (Fig 2H). Similar results were observed in F4/80$^+$ splenic macrophages in EPOR-C mice (Fig 2I) and APP/PS1-21 mice (Fig 2J and K) *in vivo*.

Collectively, these data demonstrate that macrophage EPO signaling plays an essential role in promoting phagocytosis, degradation, and the inflammatory response during the clearance of $A\beta$ *in vitro* and *in vivo*.

EPO promotes $A\beta$ clearance via PPARγ in macrophages

Regarding possible mechanisms we hypothesized that EPO signaling may promote $A\beta$ clearance through PPARγ, as accumulated evidence shows that PPARγ enhances the clearance of soluble $A\beta$ by myeloid cells (Cramer *et al*, 2012; Mandrekar-Colucci *et al*, 2012).

To test this idea, we first detected whether EPO increased levels of PPARγ and scavenger receptor A (SRA) which is a well-known target of PPARγ-mediated gene expression and has been indicated as an important receptor for $A\beta$ phagocytosis (Khan *et al*, 2019). In the presence of $A\beta_{42}$, rhEPO dose-dependently increased the protein amounts of PPARγ and SRA (Fig 3A), but genetic deletion of Epor reduced their levels in PMs *in vitro* (Fig 3B). Pre-treatment with rhEPO for 24 h greatly increased protein levels of PPARγ and SRA in F4/80$^+$ splenic macrophages in WT mice (Fig 3C), but their levels were reduced by ~80 and 60% in EPOR-MKO mice, respectively (Fig 3D). Moreover, pre-treatment with rhEPO also enhanced levels of PPARγ and SRA in F4/80$^+$ splenic macrophages in APP/PS1-21 mice (Fig 3E), but the depletion of EPOR in macrophages decreased their levels in APP/PS1-21 mice (Fig 3F). Furthermore, we also observed that $A\beta_{42}$ increased levels of PPARγ and SRA in macrophages *in vitro* and *in vivo* (Fig EV2H–J), that was in line with $A\beta_{42}$'s ability to induce EPO signaling. Therefore, these data suggested that EPO enhanced PPARγ expression in macrophages *in vitro* and *in vivo*.

GW9662 (GW, a selective antagonist for PPARγ) abolished EPO-increased $A\beta_{42}$ phagocytosis in macrophages (Fig 3G); rosiglitazone (RSG, a PPARγ agonist) still significantly enhanced $A\beta_{42}$ engulfment in *Lyz2-Cre$^{+/+}$/Epor$^{loxp/loxp}$* PMs *in vitro* (Fig 3H), both of which support that EPO promoted Aβ42 engulfment through PPARγ. Similar results were observed *in vivo* when GW or RSG was pre-given to WT mice (Fig 3I and J) or APP/PS1-21 mice (Fig 3K and L). Together these data indicate that EPO increases $A\beta_{42}$ removal by inducing PPARγ expression in macrophages.

GW abolished EPO-reduced expression of TNF-α and IL-1β and EPO-induced IL-10 expression in PMs *in vitro* (Fig 3M). RSG also reduced levels of TNF-α and IL-1β, and increased levels of IL-10 in EPOR-deficient macrophages (Fig 3M). Similar results were also observed *in vivo* in F4/80$^+$ splenic macrophages in EPOR-C mice and APP/PS1-21 mice (Fig 3N and O). Taken together, these observations suggest that EPO mainly suppress $A\beta_{42}$-induced inflammatory response through PPARγ in macrophages.
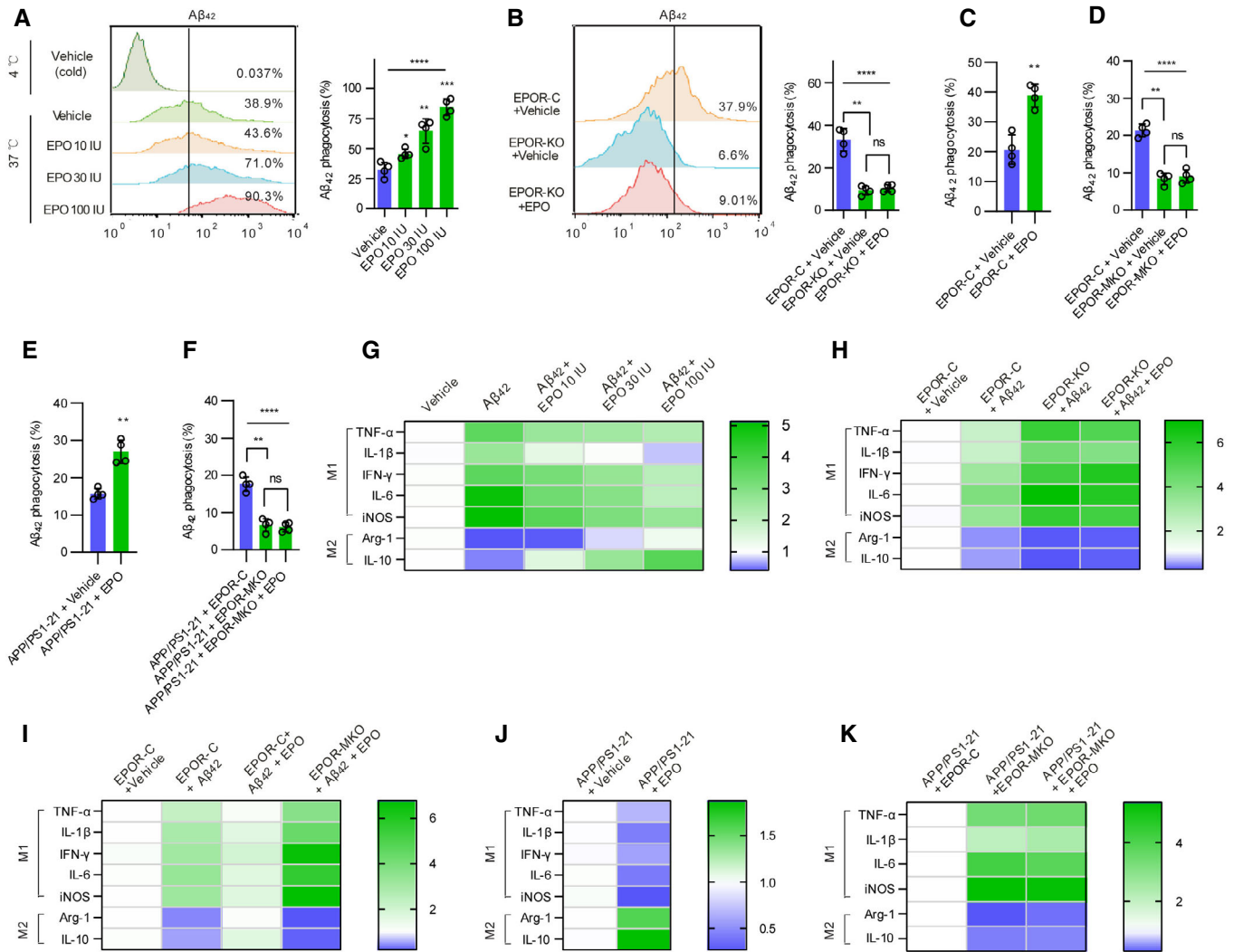
Figure 2. EPO promotes macrophage clearance of Aβ and suppresses Aβ-induced inflammatory response.

A   PMs treated with EPO of indicated concentration were measured by flow cytometry (*n* = 4). Vehicle (cold) was macrophage treated with PBS incubated at 4°C. It was used as a negative control to exclude Aβ bound with macrophage from Aβ engulfment. Vehicle was macrophage treated with PBS incubated at 37°C as control.

B   PMs from *Lyz2-Cre*$^{+/+}$/*Epor*$^{loxp/loxp}$ mice (EPOR-MKO) or *Lyz2-Cre*$^{+/+}$/*Epor*$^{+/+}$ mice (EPOR-C) were treated with PBS (Vehicle) or rhEPO for 12 h and then applied for Aβ phagocytosis assay.

C–F   F4/80$^+$CD11b$^+$ splenic macrophages from PBS (Vehicle) or rhEPO (10,000 IU/kg/day, i.p., twice per day for 1 day) treated EPOR-C mice (C), or EPOR-MKO mice (D), or from rhEPO (5,000 IU/kg, i.p., every second day for 5 days) treated APP/PS1-21 mice (5 months) (E), or from APP/PS1-21+EPOR-MKO mice (*APP/PS-1-21*$^{+/+}$/*Lyz2-Cre*$^{+/+}$/*Epor*$^{loxp/loxp}$, 5 months) (F) were purified for Aβ$_{42}$ phagocytosis assay (*n* = 4).

G, H   PMs from (A, B) were treated with PBS (Vehicle) or rhEPO for 12 h, then with Aβ$_{42}$ (5 μM) for another 12 h and applied for detection of inflammatory factor expression by QPCR (*n* = 4).

I–K   Macrophages from (C–F) were applied for detection of inflammatory factor expression by QPCR (*n* = 4). Vehicle (H, I) is Aβ resolution and Vehicle (J) is PBS.

Data information: For multiple groups, one-way ANOVA was used. Unpaired *t*-tests were used for the comparison of two groups. Results are presented as mean ± s.d., *$P < 0.05$, **$P < 0.01$, ***$P < 0.001$ and ****$P < 0.0001$; ns denotes no statistical significance. QPCR, quantitative polymerase chain reaction. EPOR-KO macrophages were PMs isolated from EPOR-MKO mice.

EPO signaling in peripheral macrophage regulates peripheral Aβ accumulation, brain Aβ efflux and brain Aβ deposition

Accumulated evidence has established that peripheral Aβ clearance contributes to regulating Aβ accumulation in the brain (Cheng *et al*, 2020). Given the important roles peripheral macrophage EPO signaling played in promoting Aβ clearance we next explored its contributions to Aβ efflux, and peripheral and central Aβ accumulation.

We first tested whether EPO promoted Aβ$_{42}$ efflux from the brain. To this end Flag-tagged Aβ$_{42}$ was injected into the lateral
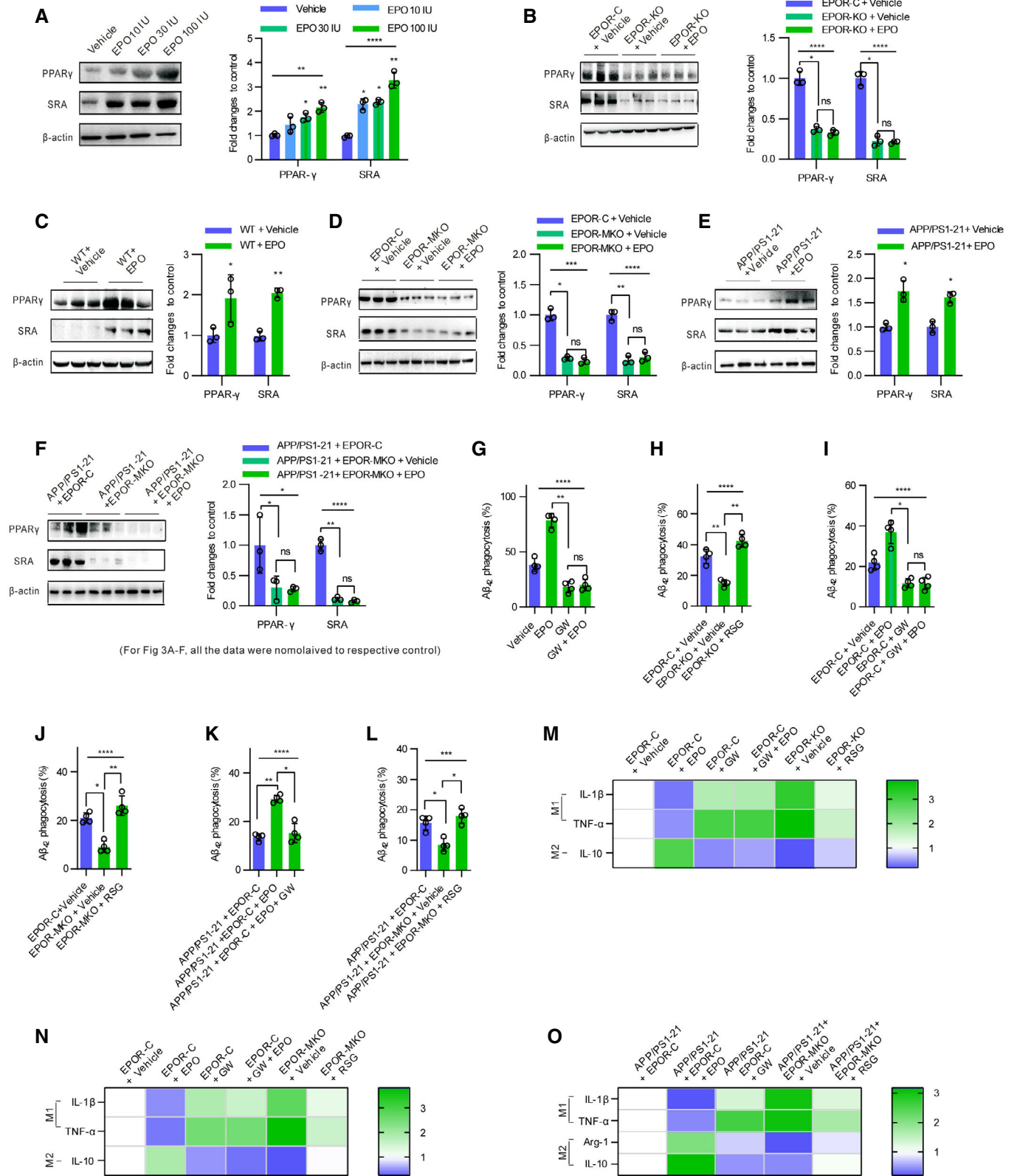
(For Fig 3A-F, all the data were nomolaived to respective control)

(For Fig 3M-O, all the data were the fold-changes relative to control)

Figure 3.

◀

ventricles of adult EPOR-C mice (Fig EV3A). After 24 h, more than two-fold increases of Flag-Aβ$_{42}$ amounts were detected in spleens of EPO-treated mice compared with that of vehicle control mice (Fig 4A and C). Correspondingly, the levels of Flag-Aβ$_{42}$ in the hippocampi, nearby the lateral ventricles, were greatly reduced in EPO-treated mice (Fig 4A), suggesting that EPO increased Aβ$_{42}$ efflux from brains with intact blood–brain barrier. EPO is best known to induce hematopoiesis and increased erythrocytes was reported to promote Aβ clearance (Brubaker *et al*, 2017). To exclude this potential disturbance, an EPO-derived peptide, ARA290, that is nonerythrogenic but retains other functions of EPO was applied to repeat above experiments (Brines *et al*, 2008). Similar effects of ARA290 (Fig 4B and C) indicated an essential contribution of nonerythropoietic activity of EPO. Furthermore, we sought to investigate the role of macrophage EPO signaling in Aβ$_{42}$ efflux. The macrophage *EPOR^{−/−}* (EPOR-MKO) mice were generated by crossing the C57BL/6 background *LysM-Cre^{+/+}* mice with *EPOR^{loxp/loxp}* mice (Luo *et al*, 2016a). Neither EPO nor ARA290 changed levels of Flag-Aβ$_{42}$ in spleens or in the hippocampi in EPOR-MKO mice (Fig 4D–F), suggesting that peripheral macrophage EPO signaling played a central role in promoting Aβ$_{42}$ efflux from brains.

Subsequently, we investigated EPO effects on peripheral and central Aβ accumulation in APP/PS1-21 mice. Following EPO or ARA290 treatment for 2 weeks, numbers of Iba1^{+} microglia surrounding Aβ plaques did not change significantly (Fig EV3B). Levels of Aβ$_{42}$ and Aβ$_{40}$ were greatly reduced in plasma (Fig EV3C) and spleen (Fig 4G) and were correspondingly decreased in brains (Fig 4H). Moreover, the deposition of Aβ in cortex and hippocampus were also greatly reduced (Fig 4I). These data indicate that the exogenous EPO or ARA290 decreased peripheral and central Aβ amounts, leading to reduced Aβ deposition in brains of APP/PS1-21 mice.

We next sought to investigate the role of peripheral macrophage EPO signaling in peripheral and central Aβ accumulation in APP/PS1-21 mice. To this end, the macrophage *EPOR^{−/−}* (*Lyz2-Cre^{+/+}/Epor^{loxp/loxp}*) mice were crossed with the APP/PS1-21 mice to get the APP/PS1-21+EPOR-MKO mice (Fig EV3D). In these mice, while the EPOR expression in splenic macrophages was greatly reduced (Fig EV3E and F), numbers of F4/80^{+} splenic macrophages did not change significantly (Fig EV3G). However, EPOR expression in Iba1^{+} microglia in brains of APP/PS1-21+EPOR-MKO mice was not significantly reduced (Fig EV3H). The deficiency of EPOR in

peripheral macrophages greatly enhanced amounts of Aβ$_{42}$ and Aβ$_{40}$ in plasma (Fig EV3I) and spleens (Fig 4J) in 5- and 11-month-old APP/PS1-21 mice. Meanwhile, amounts of Aβ$_{42}$ and Aβ$_{40}$ in brains were correspondingly increased in APP/PS1-21+EPOR-MKO mice compared with that of age- and sex-matched APP/PS1-21+EPOR-C mice (Fig 4K). Furthermore, the deposition of Aβ in cortex and hippocampus were more evident in APP/PS1-21+EPOR-MKO mice (Fig 4L and M). Together these data indicate that the endogenous peripheral macrophage EPO signaling may play an important role in reducing peripheral and central Aβ amounts, leading to reduced Aβ deposition in brains of APP/PS1-21 mice.

Erythropoietin receptor expression has also been reported in central macrophages (Tamura *et al*, 2017), and lysozyme M-Cre-lox recombination targets cells of the myeloid lineage (Luo *et al*, 2016a), including microglia. To avoid the potential contributions of central macrophage EPOR signaling to brain Aβ clearance, we established a bone marrow transplantation (BMT) model to further confirm the role of peripheral macrophage EPO signaling (Fig 4N). The transplantation of bone marrow cells (BMCs) from EPOR-MKO mice to APP/PS1-21 transgenic mice resulted in reduced protein amounts of EPOR, p-JAK2, PPARγ and SRA (Fig EV3J), and decreased phagocytosis of Aβ$_{42}$ and Aβ$_{40}$ (Fig 4O) in F4/80^{+} splenic macrophages compared with APP/PS1-21 mice received BMCs from EPOR-C mice. However, EPOR levels in Iba1^{+} macrophage/microglia in brains were not reduced, indicating a specific depletion of EPOR in peripheral macrophages (Fig EV3K). Meanwhile, levels of Aβ in plasma (Fig EV3L) and spleens (Figs 4P and EV3M) were significantly increased, so were amounts of Aβ$_{42}$ and Aβ$_{40}$ in brains (Fig 4Q). Furthermore, the deposition of Aβ in cortex and hippocampus were more evident in APP/PS1-21 mice received BMCs from EPOR-MKO mice (Fig 4R). Therefore, these data indicate that the endogenous peripheral macrophage EPO signaling regulates peripheral Aβ accumulation, brain Aβ efflux and central Aβ deposition.

Peripheral macrophage EPOR-deficient exacerbates brain AD-type pathologies and behavioral deficits in APP/PS1-21 mice

Consequently, we investigated whether EPOR-depletion in peripheral macrophages aggravated pathological and behavioral changes in APP/PS1-21 mice. Compared with APP/PS1-21+EPOR-C mice, APP/PS1-
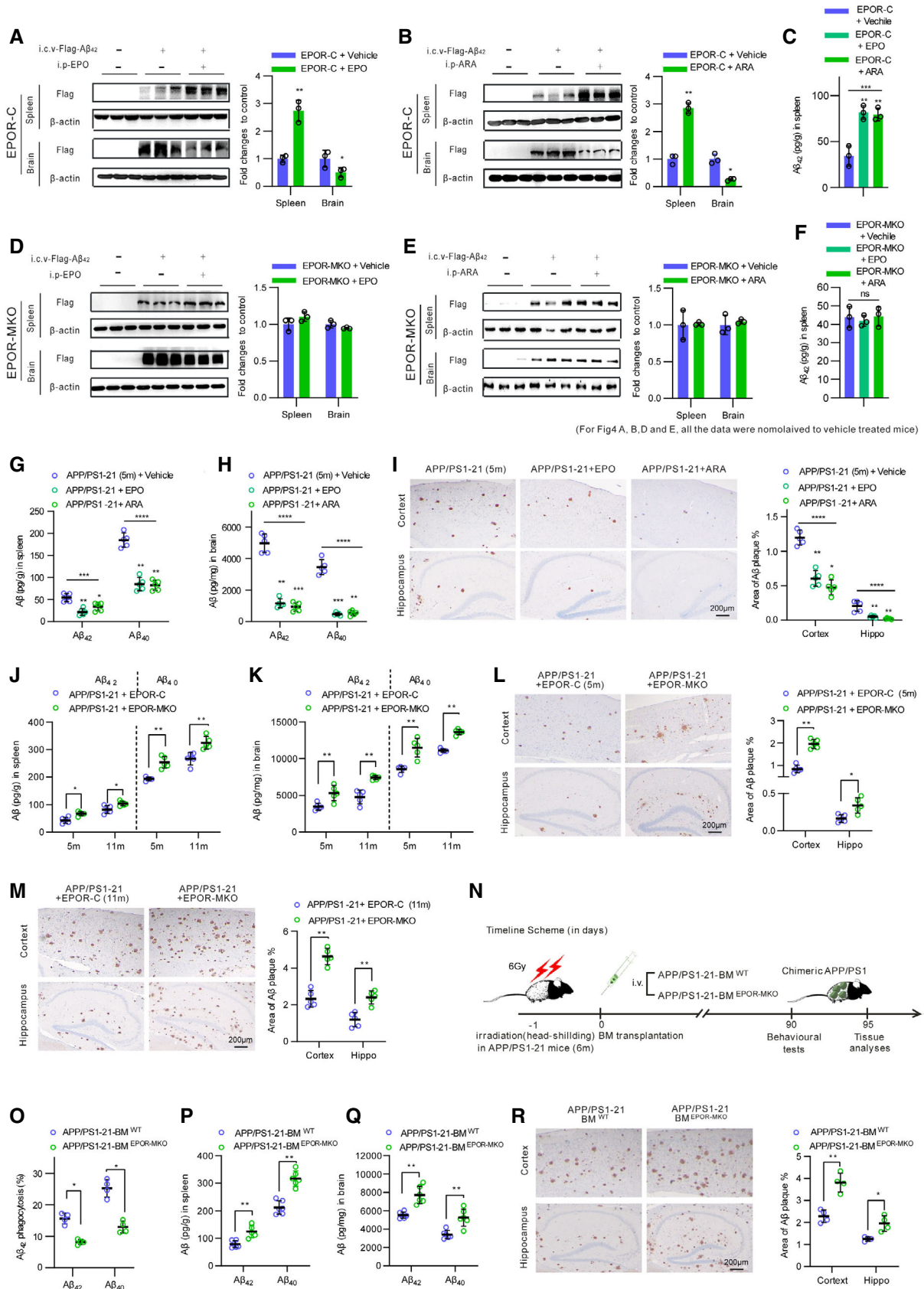
Figure 4.

21+EPOR-MKO mice exhibited more severe neuroinflammation in the cortex and the hippocampus, as reflected by increased levels of TNF-α, IL-1β, IL-6 and iNOS, and decreased amounts of Arg-1 and IL-10 (Fig 5A and B). Moreover, we also observed more dendrites damage and apoptosis, as reflected by MAP-2, and TUNEL staining in the hippocampus of 11-month-old APP/PS1-21+EPOR-MKO mice (Fig EV4A). For non-cognitive behavioral deficits, we observed a great reduction in nesting and social interactive behaviors in 5-month-old APP/PS1-21+EPOR-MKO mice (Fig 5C). For 11-month-old APP/PS1-21+EPOR-MKO mice, more severe non-cognitive and cognitive behavioral deficits, as reflected by different assays including Morris water maze test were observed (Fig 5D and E).

Next, we applied the above established BMT model to confirm the contributions of peripheral macrophage EPO signaling. Compared with APP/PS1-21 mice received BMCs from EPOR-C mice, APP/PS1-21 mice received BMCs from EPOR-MKO mice exhibited more severe neuroinflammation in the cortex and the hippocampus (Fig 5F), more dendrites damage and apoptosis, as reflected by MAP-2 and TUNEL staining in the hippocampus (Fig EV4B), and more severe non-cognitive and cognitive behavioral deficits (Fig 5G and H).

Together, these observations demonstrate that peripheral macrophage EPO signaling regulates peripheral Aβ accumulation, brain Aβ efflux and central Aβ deposition and behavioral deficits in APP/PS1-21 mice.

EPO and ARA290 improve impaired EPO signaling and dysregulated functions of peripheral macrophages in old APP/PS1-21 mice

Recent observations indicate that functions of peripheral macrophages are also dysregulated in response to Aβ (Famenini *et al*, 2017; Fiala *et al*, 2017). Therefore, we next explored whether EPO signaling contributed to the dysregulated immune response of peripheral macrophages to Aβ in APP/PS1-21 mice.

After our above data showed enhanced EPO signaling in F4/80[+] spleen macrophages from 6-week-old APP/PS1-21 mice (Fig 1H), we found that in older, 5- and 11-month-old APP/PS1-21 mice, protein amounts of EPO, EPOR, p-JAK2, PPARγ and SRA were greatly reduced in F4/80[+] spleen macrophages (Fig 6A and B), indicating impaired EPO signaling of peripheral macrophages in old APP/PS1-

21 mice. Moreover, the phagocytosis of Aβ$_{42}$ (Fig 6C and D), and the expression of IDE and NEP (Fig 6E) were significantly decreased but the inflammatory response to Aβ$_{42}$ (Fig 6F) was increased in F4/80[+] spleen macrophages of 5- and 11-month-old APP/PS1-21 mice, suggesting dysregulated response of peripheral macrophages to Aβ$_{42}$.

However, pre-treatment with rhEPO or nonerythrogenic EPO analogue ARA290 significantly enhanced protein amounts of EPOR, p-JAK2, PPARγ and SRA in F4/80[+] spleen macrophages of 11-month-old APP/PS1-21 mice compared with vehicle controls (Fig 6G). Correspondingly, the phagocytosis of Aβ$_{42}$ (Fig 6H), the expression of IDE and NEP (Fig 6I), and the inflammatory response to Aβ$_{42}$ (Fig 6J) of F4/80[+] spleen macrophages were also greatly improved by EPO and ARA290. Therefore, our results indicate an important contribution of impaired EPO signaling to dysregulated functions of peripheral macrophages in old APP/PS1-21 mice.

While our above data indicate that Aβ$_{42}$ induces macrophage EPO signaling to promote its clearance (Figs 1A–E and EV1A–J), the aging of transgenic AD model mice are accompanied with increased Aβ levels. So, we hypothesized that higher concentrations of Aβ$_{42}$ may impaired macrophage EPO signaling. Protein amounts of Aβ$_{42}$ and Aβ$_{40}$ in plasma (Fig EV4C) and spleen (Fig EV4D and E) were significantly enhanced in an age-dependent way in APP/PS1-21 mice. *In vitro*, while 5 μM Aβ$_{42}$ significantly induced EPO signaling, 7.5 and 10 μM Aβ$_{42}$ greatly decreased EPO related molecules expression in macrophages (Fig 6K), and 10 μM Aβ$_{42}$ decreased macrophage phagocytosis of Aβ$_{42}$ and Aβ$_{40}$ (Fig 6L), and decreased expression of IDE and NEP (Fig 6M). In addition, higher inflammatory response to Aβ$_{42}$ was observed in macrophages treated with 10 μM Aβ$_{42}$ compared with 5 μM Aβ4$_2$-treated macrophages (Fig EV4F). These data suggest that high concentrations of Aβ$_{42}$ impairs EPO signaling and contributes to dysregulated functions of peripheral macrophages.

EPO and ARA290 ameliorate peripheral and central Aβ accumulation, brain AD-type pathologies and behavioral deficits in old APP/PS1-21 mice

Given the important roles of EPO in normalizing dysregulated functions of peripheral macrophages in old APP/PS1-21 mice we further
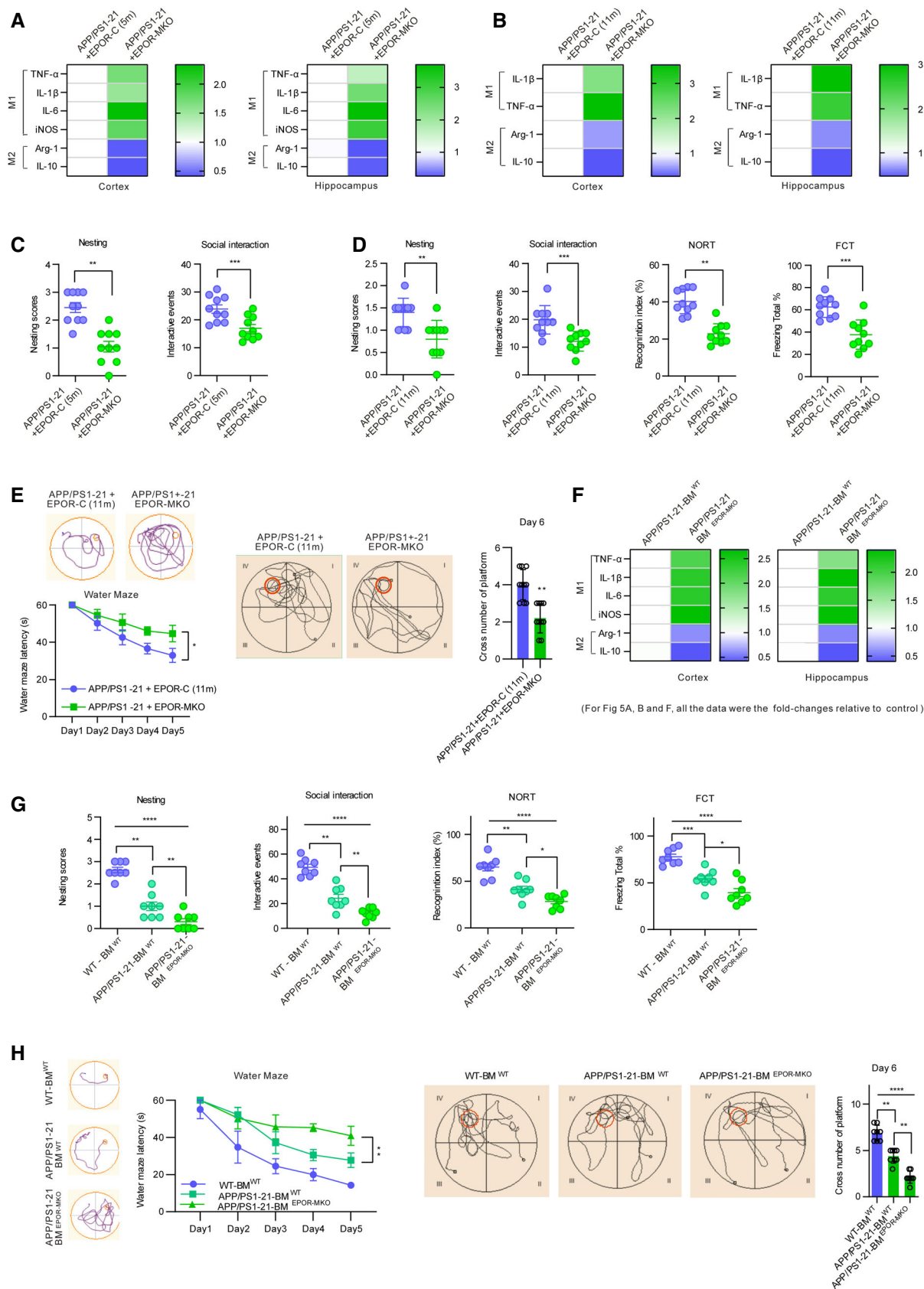
Figure 5.

◄

Figure 5. Peripheral macrophage EPOR-deficiency exacerbates brain inflammation and behavioral deficits in APP/PS1-21 mice.

A, B   Cortex and hippocampus taken from Fig 4L and M ($n = 5$) were applied for detection of inflammatory factor expression.
C–E   Non-cognitive behavioral impairments of APP/PS1-21 mice (5 months) in Fig 4L were analyzed by nest construction assay and social interaction assay (C) ($n = 10$). Both non-cognitive and cognitive behavioral impairments of APP/PS1-21 mice (11 months) in Fig 4M were analyzed by nest construction assay, social interaction assay, NORT, FCT and Morris water maze test (D, E) ($n = 10$).
F   Cortex and hippocampus were taken from APP/PS1-21 mice in Fig 4N ($n = 6$) and applied for detection of inflammatory factor expression.
G, H   Behavioral impairments APP/PS1-21 of mice in Fig 4N and WT-BM[EPOR-C] mice (irradiated WT mice transplanted with EPOR-C bone marrow cells) were analyzed by nest construction assay, social interaction assay, NORT, FCT and Morris water maze test ($n = 8$).

Data information: For multiple groups, one-way ANOVA was used. Unpaired *t*-tests were used for the comparison of two groups. Results are presented as mean ± s.d., *$P < 0.05$, **$P < 0.01$, ***$P < 0.001$ and ****$P < 0.0001$; ns denotes no statistical significance. NORT, novel object recognition test; FCT, fear conditioning test.

investigated effects of rhEPO and ARA290 on Aβ accumulation, brain AD-type pathologies and behavioral deficits in 11-month-old APP/PS1-21 mice (Fig 7A). Following EPO or ARA290 treating, levels of Aβ$_{42}$ and Aβ$_{40}$ were greatly reduced in plasma (Fig 7B), in spleens (Fig 7C) and in brains correspondingly (Fig 7D). Moreover, the deposition of Aβ in cortex and hippocampus were greatly reduced (Fig 7E). Furthermore, EPO decreased Aβ levels in APP/PS1-21 mice without altering expression of APP, NICA, BACE or PEN2 in brains (Fig EV5A), which rules out possible effects from reduction in APP expression or BACE1/g-secretase activity changes. These data indicate that the exogenous EPO or ARA290 decreased peripheral and central Aβ amounts, leading to reduced Aβ deposition in brains of old APP/PS1-21 mice.

In line with the reduced Aβ amounts, APP/PS1-21 mice received rhEPO or ARA290 treating exhibited less severe neuroinflammation (Fig 7F), less dendrites damage and apoptosis in the hippocampus and cortex (Figs 7G and EV5B), as well as less severe non-cognitive and cognitive behavioral deficits (Fig 7H and I). In addition, while rhEPO greatly induced hematopoiesis, ARA290 did not stimulate hematopoiesis during treatment (Fig EV5C).

Together, these observations demonstrate that rhEPO and ARA290 reduced peripheral and central Aβ accumulation and alleviates brain AD-type pathologies and behavioral deficits in old APP/PS1-21 mice.

Discussion

Our data here reveal that the deficiency of EPO signaling in peripheral macrophages impairs systemic Aβ clearance and deteriorates the progression of AD in mice. Specifically, this study here advances several concepts in the understanding of Aβ clearance. First, our work here reveals a feedback cascade involving the Aβ$_{42}$/EPO signaling in peripheral macrophages to regulate Aβ levels. While Aβ has long been considered as functionless and being the prime suspect for driving the development of AD, recent research shows that Aβ is an ancient, highly conserved molecule and may has crucial multifunctional physiological roles, such as regulating learning and memory, angiogenesis, neurogenesis, repairing leaks in the blood–brain barrier, promoting recovery from injury, etc. (Kent *et al*, 2020). Particularly, recent findings indicate that Aβ functions as an antimicrobial peptide and suggest Aβ deposition may be a protective innate immune response to infection. Moir *et al* (2018) revealed that Aβ expression was upregulated following viral or bacterial exposure. Moreover, Aβ generation and Aβ oligomerization appeared to mediate a diverse range of protective functions against infection, including antibiotic-like microbial killing and immuno-

modulating activities (Kumar *et al*, 2016; Eimer *et al*, 2018; Gosztyla *et al*, 2018). However, owing to the cytotoxic and immunostimulatory activity of Aβ, the ongoing Aβ generation and deposition induced by real or incorrectly perceived infection may drive inflammation, leading to pathology and widespread cell death. Therefore, it is reasonable to speculate that the host need to evolute feedback cascade to regulate Aβ levels and its-induced inflammation. In line with this speculation, our work here identified Aβ-induced macrophage EPO signaling dose-dependently promoted Aβ clearance and suppressed Aβ-activated inflammation (Figs 1 and 2). Furthermore, our recent findings together with previous reports have revealed EPO as an endogenous pro-resolving molecule that promotes the clearance of bacterial and apoptotic cells by macrophages and exerts direct cyto-protection on a variety of type of nonhematopoietic cells, including neurons (Urena-Guerrero *et al*, 2020), indicating that Aβ-induced macrophage EPO signaling may also help to clear bacterial and prevent Aβ-induced cytotoxicity. Indeed, EPO has been reported to protect neurons (Zhi-Kun *et al*, 2012) and microglia (Shang *et al*, 2012) from Aβ-induced apoptosis. Therefore, our data here together with known evidence suggest that Aβ-induced macrophage EPO signaling may be a feedback mechanism that limits Aβ's toxicity while boosts Aβ's physiological functions. Nevertheless, whether macrophage EPO signaling contributes to Aβ's physiological functions, such as antibacterial activity, remain largely unknown. Future studies are needed to address this topic.

Our results here also uncover a crucial contribution of peripheral tissue resident macrophages to clear Aβ. Accumulated findings have revealed that Aβ clearance in the periphery contributes substantially to reducing Aβ deposition in the brain (Xiang *et al*, 2015; Jin *et al*, 2017; Costa-Marques *et al*, 2019). Mounting evidence has demonstrated that phagocytosis via monocytes and macrophages is one of the predominant mechanisms of peripheral clearance of cerebral Aβ in AD (Koronyo-Hamaoui *et al*, 2020; Li *et al*, 2020a). However, existing research was most focused on contributions of circulating monocytes and the cerebral infiltrated monocytes to Aβ removal roles played by peripheral tissue macrophages to Aβ clearance remain largely unknown. Here we found that EPO increased peripheral macrophage (PMs, F4/80[+] splenic macrophages) clearance of Aβ; deficiency of EPOR in peripheral macrophages impaired the clearance of Aβ *in vitro*; depletion of peripheral macrophage EPOR by Lyz2-mediated gene KO or BMT reduced the peripheral macrophage clearance of Aβ *in vivo*, increased peripheral Aβ levels, enhanced brain Aβ deposition and exacerbated brain AD-type pathologies and behavioral deficits in APP/PS1-21 mice. Moreover, EPOR is absent in monocytes and neutrophils (Luo *et al*, 2016a), but detected in various peripheral tissue macrophages, including PMs, red pulp macrophages, Kupffer cells (Gilboa *et al*, 2017),
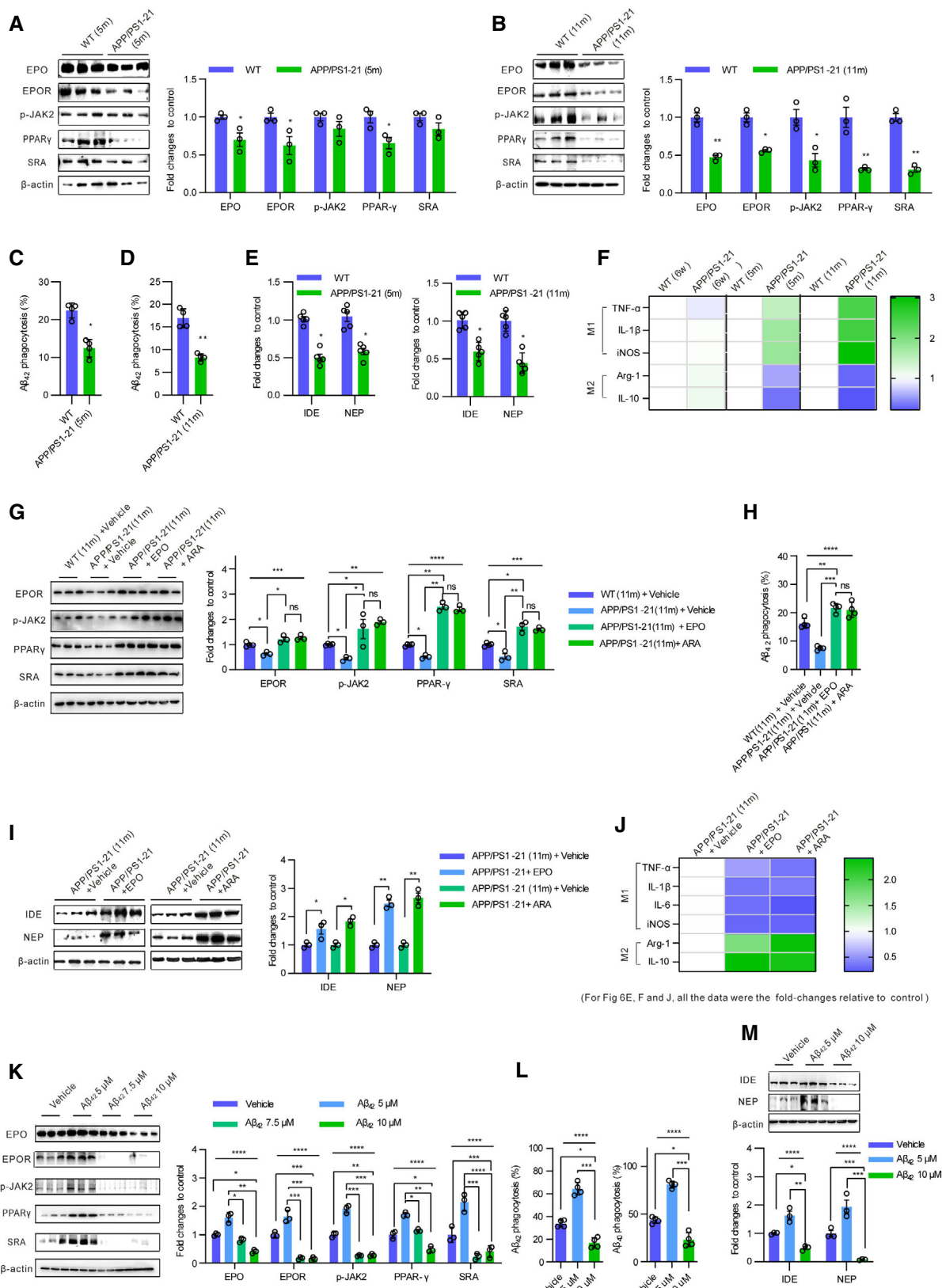
Figure 6.

Figure 6. EPO and ARA290 restore EPO signaling and dysregulated functions of peripheral macrophages in old APP/PS1-21 mice.

A–E Splenic macrophages from APP/PS1-21 (5- or 11-month-old) or matched WT mice were detected by immunoblotting with the indicated antibodies ($n = 3$) (A, B). Their phagocytosis of $A\beta_{42}$ (C, D) were measured by flow cytometry ($n = 4$). The mRNA levels of IDE and NEP were measured by QPCR ($n = 4$) (E).

F Splenic macrophages from APP/PS1-21 mice at different ages were purified for detection of inflammatory factor expression ($n = 6$).

G–J Old APP/PS1-21 mice (11 months) and WT mice at the same age were treated with rhEPO (10,000 IU/kg/day), ARA290 (0.03 mg/kg/day) or vehicle (i.p., once a day, for 14 days). Splenic macrophages were isolated for detection by immunoblotting with the indicated antibodies ($n = 3$) (G). Phagocytosis of $A\beta_{42}$ by the splenic macrophages was measured by flow cytometry ($n = 4$) (H). Protein levels of IDE and NEP were detected by immunoblotting with indicated antibodies ($n = 3$) (I). The mRNA levels of inflammatory factors were measured by QPCR ($n = 5$) (J).

K–M PMs were treated with $A\beta_{42}$ (0, 5, 7.5 or 10 μM) for 12 h, and cell lysates were detected by immunoblotting with the indicated antibodies ($n = 3$) (K). Phagocytosis of $A\beta_{42}$ and $A\beta_{40}$ was measured by flow cytometry ($n = 4$) (L). Protein levels of IDE and NEP were detected by immunoblotting with indicated antibodies ($n = 3$) (M).

Data information: All the vehicles of Fig 6 were PBS. For multiple groups, one-way ANOVA was used. Unpaired *t*-tests were used for the comparison of two groups. Results are presented as mean ± s.d., *$P < 0.05$, **$P < 0.01$, ***$P < 0.001$ and ****$P < 0.0001$; ns denotes no statistical significance. IDE, insulin degrading enzyme; NEP, neprilysin.

Source data are available online for this figure.

erythroblastic island macrophages (Li *et al*, 2019), wound skin macrophages (Haroon *et al*, 2003), lung tissue-resident macrophages (Li *et al*, 2020b) and more, suggesting that abovementioned effects were mainly owing to EPO activity in peripheral tissue macrophages. In addition, Kupffer cells were reported to be involved in Aβ clearance in AD patients (Brubaker *et al*, 2017), which was in line with EPOR's expression in Kupffer cells. Collectively, these evidence not only identify a physiological role for peripheral tissue macrophage EPO signaling in promoting Aβ clearance but also uncover the crucial role of peripheral tissue macrophages in systemic Aβ clearance. In addition, we also observed a dysregulated response of peripheral tissue macrophages to $A\beta_{42}$ in old APP/PS1-21 mice, as reflected by reduced phagocytosis of $A\beta_{42}$ and the expression of IDE and NEP but increased inflammatory response to $A\beta_{42}$ in red pulp F4/80$^+$ macrophages. Meanwhile it is also possible that macrophage EPO signaling may affect Aβ clearance via a more indirect mechanism requiring additional cell types, as tissue macrophages can alter the function of surrounding cells, via such as changed release of inflammatory mediators. Moreover, recent studies have shown that complement C3b-mediated adherence to erythrocytes can facilitate clearance and degradation of circulating Aβ (Brubaker *et al*, 2017), suggesting that EPO induced erythropoiesis may help Aβ clearance. To exclude this potential disturbance, an EPO-derived peptide, ARA290, that is nonerythrogenic but retains other functions of EPO was further applied in our experiments. In AD patients, while peripheral blood-derived macrophages have been reported to demonstrate ineffective phagocytosis of Aβ compared with the age-matched control subjects (Jairani *et al*, 2019; Krishnan *et al*, 2020), contributions of peripheral tissue

macrophages to the development of human AD and therapeutic effects of targeting peripheral tissue macrophages in treating human AD warrants further investigation.

Our work also provides clear evidence for the involvement of EPO in regulating the immune-suppressive Aβ clearance by peripheral macrophages. While our previous data showed that EPO promoted macrophage phagocytosis of apoptotic cells and bacterial (Luo *et al*, 2016a; Liang *et al*, 2021) the removal of Aβ is different from apoptotic cell and bacterial phagocytosis by recognition, uptake, and degradation of particles, leading to very different outcomes (Sole-Domenech *et al*, 2016). Here our data also showed that EPO promoted Aβ clearance and suppressed Aβ-induced inflammatory response (Fig 2). Moreover, the depletion of peripheral macrophage EPOR by Lyz2-mediated gene KO or BMT increased peripheral Aβ levels, enhanced brain Aβ deposition and exacerbated brain AD-type pathologies and behavioral deficits in APP/PS1-21 mice, indicating an essential role of peripheral macrophage EPO signaling in regulating systemic Aβ levels in AD model mice. Furthermore, we also identified that EPO signaling in peripheral macrophages was impaired in old AD model mice and pharmacological interference in EPO signaling normalized the impaired EPO signaling in peripheral macrophages, greatly improved dysregulated response of peripheral macrophages to $A\beta_{42}$, reduced peripheral Aβ levels, decreased brain Aβ deposition and ameliorated brain AD-type pathologies and behavioral deficits in APP/PS1-21 mice. Although previous studies showed that EPO improved outcomes of AD, underlying mechanisms are not fully understood. Our investigations here suggest that EPO improves the peripheral macrophage phagocytic defect in AD model mice. However, the contribution of

Figure 7. EPO and ARA290 ameliorate peripheral and central Aβ accumulation, brain AD-type pathologies and behavioral deficits in old APP/PS1-21 mice.

A Timeline of rhEPO (10,000 IU/kg/day) or ARA290 (0.03 mg/kg/day) treatments of old APP/PS1-21 mice (11 months) ($n = 5$).

B Plasma Aβ levels were measured by ELISA ($n = 5$).

C, D Soluble Aβ levels in spleens (C) and brains (D) were measured by ELISA ($n = 5$).

E Aβ plaques in the cortex and hippocampus ($n = 5$) were detected by IHC.

F Cortex and hippocampus were taken, and the mRNA levels of inflammatory factors were measured by QPCR ($n = 5$).

G Expression of MAP-2 or the apoptotic neurons of hippocampus were detected by IF staining and then statistically quantified ($n = 5$).

H, I Both non-cognitive and cognitive behavioral impairments were analyzed by nest construction assay, social interaction assay, NORT, FCT and Morris water maze test ($n = 10$).

Data information: All the vehicles of Fig 7 were PBS. For multiple groups, one-way ANOVA was used. Unpaired *t*-tests were used for the comparison of two groups. Results are presented as mean ± s.d., *$P < 0.05$, **$P < 0.01$, ***$P < 0.001$ and ****$P < 0.0001$; ns denotes no statistical significance. IF, Immunofluorescent; MAP-2, microtubule-associated protein 2; NeuN, neuronal nuclei; TUNEL, terminal dUTP nick end labeling.
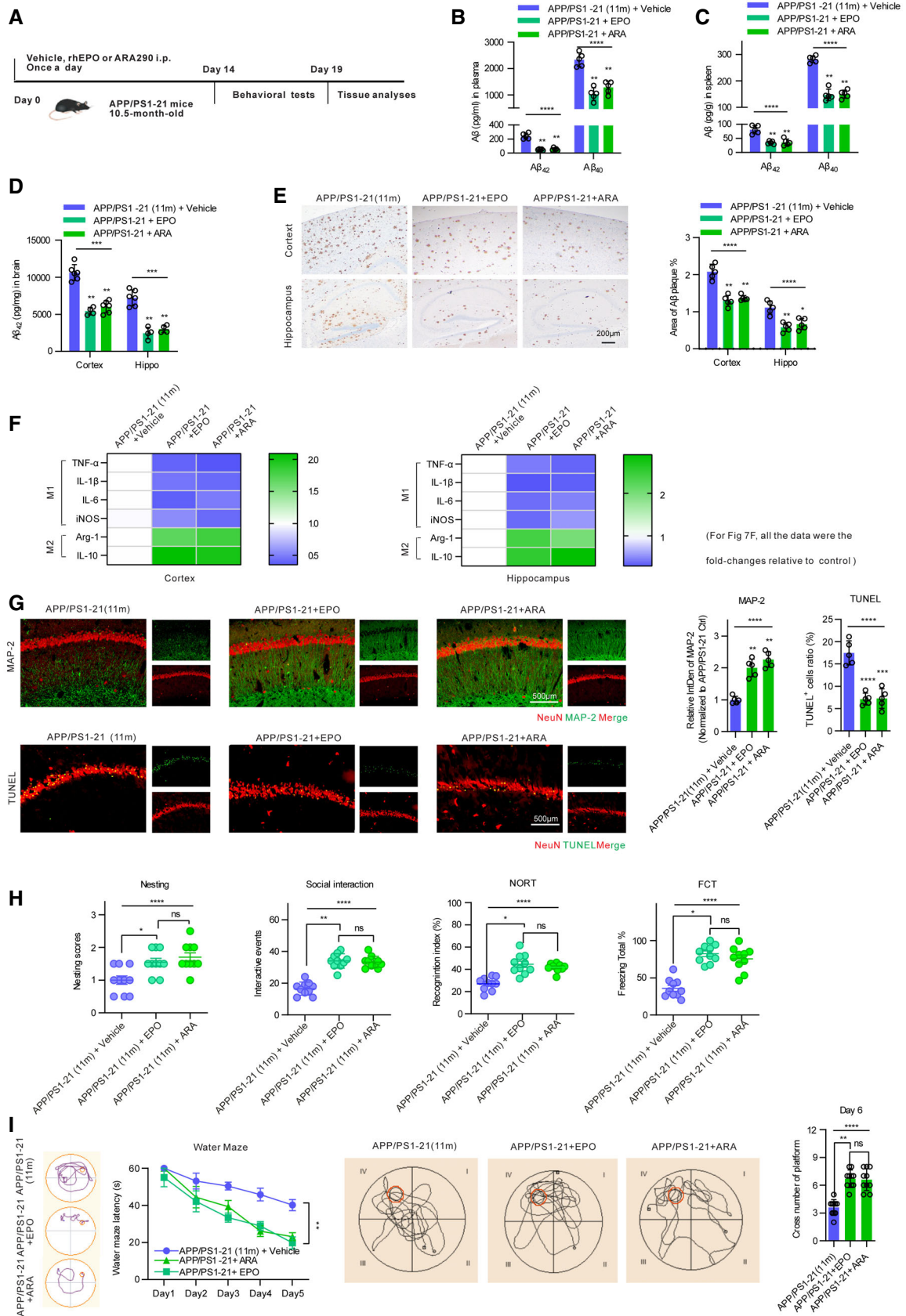
Figure 7.

peripheral macrophage EPO signaling to the development of human AD and its potential therapeutic use warrants further investigations.

Materials and Methods

Animals

C57BL/6 wild-type mice were purchased from Animal Core Facility of Nanjing Medical University. The C57BL/6 background myeloid-specific *EPOR* (Luo *et al*, 2016b) knockout mice were generated as described previously and the *Lyz2-Cre$^{+/+}$/Epor$^{loxp/loxp}$*, *Lyz2-Cre$^{+/+}$/Epor$^{+/+}$* littermates were referred to as *EPOR-MKO* or *EPOR-C* mice, respectively. APP/PS1-21 mice (Xu *et al*, 2021) were provided by Prof. M. Jucker (University of Tuebingen, Germany). For the generation of APP/PS1-21+EPOR-MKO mice, EPOR-MKO mice were crossed with APP/PS1-21 mice. Male EPOR-MKO mice (8 weeks), EPOR-C mice (8 weeks), APP/PS1-21 mice (6, 5 and 11 months), APP/PS1-21+EPOR-MKO mice (5 and 11 months) and APP/PS1-21+EPOR-C mice (5 and 11 months) were age and sex matched for experiments. Five to six animals were housed per cage under specific pathogen-free (SPF) conditions with soft bedding under controlled temperature ($22°C \pm 2°C$) and photoperiods (12:12 h light/dark cycle). All experimental protocols and procedures were approved and licensed by Nanjing Medical University Animal Care and Use Committee in accordance with the National Institutes of Health guide for the care and use of Laboratory animals (approval number: 1904008). For experimental treatments, simple randomization was used to assign animals to each group. The behavioral and neuropathological experiments and analysis were performed, and the raw data were originally evaluated by researchers who were blinded to the animal grouping or treatments.

Reagents and antibodies

Human Aβ_{42}, Aβ_{40} and Flag-Aβ_{42} were obtained from China Peptides (Shanghai, China). Hilyte-labeled Aβ was from AnaSpec (Fremont, CA, USA). Recombinant human EPO (rhEPO) was from Sunshine Pharmaceutical (Shenyang, China). ARA290, GW9662 and rosiglitazone (RSG) were from MCE (Monmouth Junction, NJ, USA). Latrunculin A was from Abcam (Cambridge, MA, USA) and Dynasore hydrate was from Sigma-Aldrich (St. Louis, MO, USA). TUNEL BrightGreen Apoptosis Detection Kit were purchased from Vazyme (Nanjing, China) and DAPI Fluoromount-GR was from Southern Biotech (Brimingham, AL, USA). Resatorvid was purchased from MCE (MedChemExpress, Plainsboro, NJ, USA). DMEM/F-12 medium (DMEM), fetal bovine serum (FBS), penicillin and streptomycin were purchased from Gibco (Waltham, MA, USA).

Antibodies against EPO (Santa Cruz, CA, USA) and PPAR-γ (CST, Boston, MA, USA) were used. Fluorescent-labeled antibodies against CD11b and F4/80 were from Invitrogen (Carlsbad, CA, USA). The other key antibodies used in the experiments were obtained from Abcam (Cambridge, MA, USA).

Isolation and culture of macrophages

Peritoneal macrophages (PMs), splenic cells and bone marrow cells were obtained and cultured as described previously (Xu

et al, 2021). Briefly, peritoneal macrophages were obtained by peritoneal lavage of mice pre-treated with 6% starch broth i.p. (1 ml per mouse). Three days later, peritoneal cell was collected. For splenic cells, spleens were filtered with 70 μm filters, and bone marrow cells were flushed from femurs and tibias of mice. Red blood cells were lysed and single-cell suspensions were cultured overnight. The purity of macrophages was evaluated with CD11b and F4/80 antibodies (1:200) by flow cytometry. F4/80$^+$ CD11b$^+$ cells were identified as macrophages in the following experiments.

Phagocytosis assays and flow cytometry

Macrophages were first incubated with Aβ (12 h) or EPO (12 h) of indicated concentrations. Hilyte-Aβ_{42} was then added to a final concentration of 1 μg/ml and incubated for 60 min at 37°C or incubated at 4°C for 60 min as negative controls. Hilyte-Aβ_{42} phagocytosis was verified by a confocal microscope (LSM800; Carl Zeiss, Jena, Germany), anti-CD11b antibody (1:1,000) was used to label the cell shape, and DAPI was used to stain the nuclei. For some experiments, cells were also treated with Latrunculin A (200 nM, 1 h), Dynasore (0.1 μM, 0.5 h), GW9662 (10 μM, 12 h) or RSG (50 μM, 12 h). Aβ phagocytosis was determined using flow cytometry as reported previously (Xu *et al*, 2021). Intracellular Aβ_{42} was quantified using ImageJ software 1.52t (Loci, Madison, WI, USA) "JACoP" plug-in. The values are represented as Pearson's correlation coefficient (Xu *et al*, 2021).

Erythropoietin receptor expression in macrophages was also determined with flow cytometry. Macrophages were incubated with EPOR antibody (1:200) for 0.5 h. For all staining, isotype controls were used. All data were analyzed using FlowJo Flow Cytometry Analysis Software (Version V10; TreeStar, Ashland, OR, USA).

Live-cell microscopy

Approximately 2.0×10^5 PMs were plated 48 h prior to imaging on a poly-D-lysine-coated glass bottom dishes (Biofil, Guangzhou, China). Twenty-four hours before imaging, media was replaced to RPMI without phenol red. Hilyte-labeled Aβ_{42} was added into the medium when imaging started. The cells were imaged on a Nikon Eclipse Ti (Zeiss LSM900) in an enclosure to maintain humidity, a temperature of 37°C and 5% CO_2. Movie was analyzed by Imaris 9.0.1 software.

Western blotting (WB) and co-immunoprecipitation (IP)

The analysis was routinely conducted according to our previous reports (Li *et al*, 2020a). Briefly, total protein was extracted from primary microphage and the brains using RIPA lysis buffer for WB analysis. Following primary antibodies were applied: EPO (1:1,000), EPOR (1:1,000), p-JAK2 (1:1,000), PPARγ (1:1,000), SRA (1:5,000), IgG (1:1,000), NICA (1:1,000), BACE (1:1,000), PEN2 (1:1,000), APP (1:1,000), IDE (1:5,000), NEP (1:1,000), Flag (1:1,000) or β-actin (1:1,000). The signals of specific protein were detected with a Gel Doc imager (Bio-Rad, Hercules, CA, USA) and given as the fraction of control β-actin.

For the co-immunoprecipitation assay, PMs were seeded into a 12-well plate at a density of 1.0×10^5. After treatment with Aβ_{42}

(5 μM) for 12 h, cells of each well were lysed by 200 μl of immuno-precipitated lysis buffer. Ten microliter of lysates was collected as an input sample. Anti-EPOR and anti-IgG were added into the remaining lysates and incubated at 4°C overnight. Subsequently, 20 μl of Protein A/G magnetic beads (MCE, NJ, USA) were added to incubate at 4°C for other 3 h. After washing and boiling, the immunoprecipitates were loaded on SDS-PAGE. The samples were electrophoretically separated on 12% SDS-PAGE gels. Following this, the proteins were transferred to PVDF membranes using Trans-Blot apparatus (Bio-Rad, Hercules, CA, USA). The membranes were blocked with Tris-buffered saline solution (TBS) containing 5% BSA for 2 h and were then incubated at 4°C overnight with primary antibodies.

ELISA and nitric oxide detection

Blood was drawn from inner canthus of each mouse and the samples were centrifuged at 4,000 rpm at 4°C for 10 min and then plasma was collected. In other experiments, protein of brain and spleen were extracted. Levels of Aβ in plasma, brain and spleen were determined with enzyme-linked immune sorbent assay (ELISA), according to the manufacturer's instructions and the Aβ level was measured as A450 nm. Supernatants from different wells were collected and a standard Griess assay (Sigma-Aldrich) was performed to analyze the production of nitric oxide (NO).

Quantitative real-time (RT)-PCR

Quantitative RT-PCR was routinely conducted as previously described in our previous reports (Li *et al*, 2020a). Briefly, total RNA was extracted with RNAiso plus Total RNA Extraction Kit (Takara, Dalian, China). PrimeScript Reverse Transcriptase (Takara, Dalian, China) was used to reverse RNA to cDNA. The relative expression of inflammatory cytokines was detected with ChamQ SYBR qPCR Master Mix (Vazyme, Nanjing, China) on the LightCycler 96 (Roche, Basel, Switzerland).

Intracerebroventricular injection (i.c.v.) Flag-Aβ

From 24 h prior to the intraventricular injection of Flag-Aβ$_{42}$, 8 weeks old EPOR-MKO and control mice were injected intraperitoneally with EPO (10,000 IU/kg/day), ARA290 (0.03 mg/kg/day) or vehicle (200 μl) i.p. for four times every 12 h ($n = 3$). Then, the intraventricular injection was performed as described previously (Wang *et al*, 2015; Qian *et al*, 2016; Xu *et al*, 2021). Twelve hours after the intraventricular injection, EPO, ARA290 or vehicle was given again, and the mice were sacrificed after another 12 h. Peripheral tissues (spleen) and brains (hippocampus) were taken for protein isolation and following western blot assays with Flag antibodies. The distribution of injected Aβ was observed by detecting the Flag-Aβ levels in spleens and brains.

Bone marrow chimeras

The recipient mice (6-month-old APP/PS1 mice) were subjected to lethal-dose irradiation (6 Gy). And 1 day later, bone marrow cells (10×10^6) derived from the tibiae and femurs of donor mice were i.v. injected into irradiated mice. After 3 months, the chimeric mice were then subjected to following experiments.

Behavioral tests

Behavioral tests, including nest construction assay, resident-intruder assay and novel object recognition test (NORT) were performed as described in our previous reports (Li *et al*, 2020a). Fear conditioning test (FCT) was conducted with a dedicated chamber (Panlab, Harvard Apparatus, Holliston, MA, USA), and the recall of fear memory was assessed by freezing time (PACKWIN 2.0.06, Harvard Apparatus, Holliston, MA, USA). Morris water maze (MWM) test was conducted in a circular tank. After 5 days of training, the probe test was then conducted. The escape latency, defined as the time taken to find the hidden platform and the number of crossing the indicated platform, was recorded and analyzed.

Immunohistochemistry (IHC) analysis

The mice were sacrificed and perfused intracardially with 4% paraformaldehyde in ice-cold PBS. The antibody of Aβ (1:100) was used for Aβ deposition. Aβ immunostaining were evaluated in the cortex and the hippocampus. Images of the hemisphere sections were captured using a Nikon Coolscope (Nikon) with fixed parameters. The cortex and the hippocampus were outlined on the images and analyzed using MetaMorph Offline 7.1 software (Molecular Devices, Toronto, Canada).

Immunofluorescence and terminal dUTP nick end labeling (TUNEL) assay

The brains were embedded in Tissue-Tek® O.C.T compound and frozen at −80°C. Specimens were then cut into 25-μm-thick sections by a freezing microtome (CM1860; Leica, Wetzlar, Germany). The sections were incubated overnight at 4°C with the following primary antibodies: EPOR (1:500), Iba1 (1:100) for activated microglia, NeuN (1:1,000) for neuron and MAP-2 (1:1,000). After washing, the sections were incubated with Alexa Fluor-conjugated secondary antibodies for 1 h at room temperature. Fluorescence intensity was used for quantification.

To detect the apoptosis of neuron in brain tissues, TUNEL Bright-Green Apoptosis Detection Kit was conducted. All procedures followed the manufacturer's instruction. Briefly, the slices were incubated with TUNEL reaction mixture at 37°C for 1 h in the dark. Then these slices were filled with NeuN antibody (1:1,000) at 4°C overnight. The nuclei were stained with DAPI. The quantification of images was analyzed with Image J software 1.52t.

Statistical analysis

GraphPad Prism 8.0 (GraphPad Software, San Diego, CA, USA) was used for statistical analysis and graphic presentation. The normality of data was tested by Kolmogorov–Smirnov test and Student's *t*-test was used for the comparison between two groups. For multiple groups, one-way ANOVA was used. All data are presented as the mean ± s.d. Two-sided *P*-values < 0.05 were defined as statistically significant.

Data availability

This study includes no data deposited in external repositories.

Expanded View for this article is available online.

Author contributions

Lu Xu: Investigation; methodology; writing – original draft; writing – review and editing. **Lei Li:** Data curation; formal analysis; methodology; writing – review and editing. **Cai-Long Pan:** Data curation; formal analysis. **Jing-Jing Song:** Data curation; formal analysis. **Chen-Yang Zhang:** Formal analysis. **Xiang-Hui Wu:** Data curation; formal analysis. **Fan Hu:** Formal analysis; methodology. **Xue Liu:** Formal analysis; methodology. **Zhiren Zhang:** Funding acquisition; writing – original draft; writing – review and editing. **Zhi-Yuan Zhang:** Supervision; funding acquisition; writing – original draft; writing – review and editing.

In addition to the CRediT author contributions listed above, the contributions in detail are:

Z-YZ and ZZ designed the experiments, obtained resources, and acquired funding. Z-YZ conducted the experiments with assistance from LX and LL. LX, LL, C-LP, J-JS, C-YZ, X-HW, FH and XL collected the data and contributed to the statistical analysis. LX, ZZ, and Z-YZ analyzed the data and wrote the manuscript. All authors read and approved the final manuscript.

Disclosure and competing interests statement

The authors declare that they have no conflict of interest.

References

Ashe KH, Zahs KR (2010) Probing the biology of Alzheimer's disease in mice. *Neuron* 66: 631–645

Baik SH, Kang S, Lee W, Choi H, Chung S, Kim JI, Mook-Jung I (2019) A breakdown in metabolic reprogramming causes microglia dysfunction in Alzheimer's disease. *Cell Metab* 30: 493–507

Brines M, Patel NS, Villa P, Brines C, Mennini T, De Paola M, Erbayraktar Z, Erbayraktar S, Sepodes B, Thiemermann C *et al* (2008) Nonerythropoietic, tissue-protective peptides derived from the tertiary structure of erythropoietin. *Proc Natl Acad Sci USA* 105: 10925–10930

Brubaker WD, Crane A, Johansson JU, Yen K, Garfinkel K, Mastroeni D, Asok P, Bradt B, Sabbagh M, Wallace TL *et al* (2017) Peripheral complement interactions with amyloid beta peptide: erythrocyte clearance mechanisms. *Alzheimers Dement* 13: 1397–1409

Cheng Y, Tian DY, Wang YJ (2020) Peripheral clearance of brain-derived Aβ in Alzheimer's disease: pathophysiology and therapeutic perspectives. *Transl Neurodegener* 9: 16

Condic M, Oberstein TJ, Herrmann M, Reimann MC, Kornhuber J, Maler JM, Spitzer P (2014) N-truncation and pyroglutaminylation enhances the opsonizing capacity of Aβ-peptides and facilitates phagocytosis by macrophages and microglia. *Brain Behav Immun* 41: 116–125

Costa-Marques L, Arnold K, Pardon MC, Leovsky C, Swarbrick S, Fabian C, Stolzing A (2019) Transplantation of bone marrow derived macrophages reduces markers of neuropathology in an APP/PS1 mouse model. *Transl Neurodegener* 8: 33

Cramer PE, Cirrito JR, Wesson DW, Lee CY, Karlo JC, Zinn AE, Casali BT, Restivo JL, Goebel WD, James MJ *et al* (2012) ApoE-directed therapeutics rapidly clear beta-amyloid and reverse deficits in AD mouse models. *Science* 335: 1503–1506

Eimer WA, Vijaya Kumar DK, Navalpur Shanmugam NK, Rodriguez AS, Mitchell T, Washicosky KJ, Gyorgy B, Breakefield XO, Tanzi RE, Moir RD (2018) Alzheimer's disease-associated beta-amyloid is rapidly seeded by Herpesviridae to protect against brain infection. *Neuron* 99: 56–63

Famenini S, Rigali EA, Olivera-Perez HM, Dang J, Chang MT, Halder R, Rao RV, Pellegrini M, Porter V, Bredesen D *et al* (2017) Increased intermediate M1-M2 macrophage polarization and improved cognition in mild cognitive impairment patients on omega-3 supplementation. *FASEB J* 31: 148–160

Fiala M, Kooij G, Wagner K, Hammock B, Pellegrini M (2017) Modulation of innate immunity of patients with Alzheimer's disease by omega-3 fatty acids. *FASEB J* 31: 3229–3239

Gengler S, Hamilton A, Holscher C (2010) Synaptic plasticity in the hippocampus of a APP/PS1 mouse model of Alzheimer's disease is impaired in old but not young mice. *PLoS One* 5: e9764

Gilboa D, Haim-Ohana Y, Deshet-Unger N, Ben-Califa N, Hiram-Bab S, Reuveni D, Zigmond E, Gassmann M, Gabet Y, Varol C *et al* (2017) Erythropoietin enhances Kupffer cell number and activity in the challenged liver. *Sci Rep* 7: 10379

Gosztyla ML, Brothers HM, Robinson SR (2018) Alzheimer's amyloid-beta is an antimicrobial peptide: a review of the evidence. *J Alzheimers Dis* 62: 1495–1506

Guo H, Zhao Z, Zhang R, Chen P, Zhang X, Cheng F, Gou X (2019) Monocytes in the peripheral clearance of amyloid-beta and Alzheimer's disease. *J Alzheimers Dis* 68: 1391–1400

Haroon ZA, Amin K, Jiang X, Arcasoy MO (2003) A novel role for erythropoietin during fibrin-induced wound-healing response. *Am J Pathol* 163: 993–1000

Heckmann BL, Teubner BJW, Tummers B, Boada-Romero E, Harris L, Yang M, Guy CS, Zakharenko SS, Green DR (2019) LC3-associated endocytosis facilitates beta-amyloid clearance and mitigates neurodegeneration in murine Alzheimer's disease. *Cell* 178: 536–551

Hernandez CC, Burgos CF, Gajardo AH, Silva-Grecchi T, Gavilan J, Toledo JR, Fuentealba J (2017) Neuroprotective effects of erythropoietin on neurodegenerative and ischemic brain diseases: the role of erythropoietin receptor. *Neural Regen Res* 12: 1381–1389

Herr B, Zhou J, Werno C, Menrad H, Namgaladze D, Weigert A, Dehne N, Brune B (2009) The supernatant of apoptotic cells causes transcriptional activation of hypoxia-inducible factor-1alpha in macrophages via sphingosine-1-phosphate and transforming growth factor-beta. *Blood* 114: 2140–2148

Jairani PS, Aswathy PM, Krishnan D, Menon RN, Verghese J, Mathuranath PS, Gopala S (2019) Apolipoprotein E polymorphism and oxidative stress in peripheral blood-derived macrophage-mediated amyloid-Beta phagocytosis in Alzheimer's disease patients. *Cell Mol Neurobiol* 39: 355–369

Jansen IE, Savage JE, Watanabe K, Bryois J, Williams DM, Steinberg S, Sealock J, Karlsson IK, Hagg S, Athanasiu L *et al* (2019) Genome-wide meta-analysis identifies new loci and functional pathways influencing Alzheimer's disease risk. *Nat Genet* 51: 404–413

Jin WS, Shen LL, Bu XL, Zhang WW, Chen SH, Huang ZL, Xiong JX, Gao CY, Dong Z, He YN *et al* (2017) Peritoneal dialysis reduces amyloid-beta plasma levels in humans and attenuates Alzheimer-associated phenotypes in an APP/PS1 mouse model. *Acta Neuropathol* 134: 207–220

Kent SA, Spires-Jones TL, Durrant CS (2020) The physiological roles of tau and Aβ: implications for Alzheimer's disease pathology and therapeutics. *Acta Neuropathol* 140: 417–447

Khan MA, Alam Q, Haque A, Ashafaq M, Khan MJ, Ashraf GM, Ahmad M (2019) Current Progress on peroxisome proliferator-activated receptor gamma agonist as an emerging therapeutic approach for the treatment of Alzheimer's disease: an update. *Curr Neuropharmacol* 17: 232–246

Koronyo-Hamaoui M, Sheyn J, Hayden EY, Li S, Fuchs DT, Regis GC, Lopes DHJ, Black KL, Bernstein KE, Teplow DB *et al* (2020) Peripherally derived angiotensin converting enzyme-enhanced macrophages alleviate Alzheimer-related disease. *Brain* 143: 336–358

Krishnan D, Menon RN, Mathuranath PS, Gopala S (2020) A novel role for SHARPIN in amyloid-beta phagocytosis and inflammation by peripheral blood-derived macrophages in Alzheimer's disease. *Neurobiol Aging* 93: 131–141

Kumar DK, Choi SH, Washicosky KJ, Eimer WA, Tucker S, Ghofrani J, Lefkowitz A, McColl G, Goldstein LE, Tanzi RE *et al* (2016) Amyloid-beta peptide protects against microbial infection in mouse and worm models of Alzheimer's disease. *Sci Transl Med* 8: 340ra372

Kunkle BW, Grenier-Boley B, Sims R, Bis JC, Damotte V, Naj AC, Boland A, Vronskaya M, van der Lee SJ, Amlie-Wolf A *et al* (2019) Genetic meta-analysis of diagnosed Alzheimer's disease identifies new risk loci and implicates Aβ, tau, immunity and lipid processing. *Nat Genet* 51: 414–430

Lane CA, Hardy J, Schott JM (2018) Alzheimer's disease. *Eur J Neurol* 25: 59–70

Li W, Wang Y, Zhao H, Zhang H, Xu Y, Wang S, Guo X, Huang Y, Zhang S, Han Y *et al* (2019) Identification and transcriptome analysis of erythroblastic island macrophages. *Blood* 134: 480–491

Li L, Wu XH, Zhao XJ, Xu L, Pan CL, Zhang ZY (2020a) Zerumbone ameliorates behavioral impairments and neuropathology in transgenic APP/PS1 mice by suppressing MAPK signaling. *J Neuroinflammation* 17: 61

Li Y, Li M, Wei R, Wu J (2020b) Identification and functional analysis of EPOR (+) tumor-associated macrophages in human osteosarcoma lung metastasis. *J Immunol Res* 2020: 9374240

Liang F, Guan H, Li W, Zhang X, Liu T, Liu Y, Mei J, Jiang C, Zhang F, Luo B *et al* (2021) Erythropoietin promotes infection resolution and lowers antibiotic requirements in *E. coli*- and *S. aureus*-initiated infections. *Front Immunol* 12: 658715

Luo B, Gan W, Liu Z, Shen Z, Wang J, Shi R, Liu Y, Jiang M, Zhang Z, Wu Y (2016a) Erythropoeitin signaling in macrophages promotes dying cell clearance and immune tolerance. *Immunity* 44: 287–302

Luo B, Wang J, Liu Z, Shen Z, Shi R, Liu YQ, Liu Y, Jiang M, Wu Y, Zhang Z (2016b) Phagocyte respiratory burst activates macrophage erythropoietin signaling to promote acute inflammation resolution. *Nat Commun* 7: 12177

Luo B, Wang Z, Zhang Z, Shen Z, Zhang Z (2019) The deficiency of macrophage erythropoietin signaling contributes to delayed acute inflammation resolution in diet-induced obese mice. *Biochim Biophys Acta Mol Basis Dis* 1865: 339–349

Mandrekar-Colucci S, Karlo JC, Landreth GE (2012) Mechanisms underlying the rapid peroxisome proliferator-activated receptor-gamma-mediated amyloid clearance and reversal of cognitive deficits in a murine model of Alzheimer's disease. *J Neurosci* 32: 10117–10128

Minhas PS, Latif-Hernandez A, McReynolds MR, Durairaj AS, Wang Q, Rubin A, Joshi AU, He JQ, Gauba E, Liu L *et al* (2021) Restoring metabolism of myeloid cells reverses cognitive decline in ageing. *Nature* 590: 122–128

Moir RD, Lathe R, Tanzi RE (2018) The antimicrobial protection hypothesis of Alzheimer's disease. *Alzheimers Dement* 14: 1602–1614

Naj AC, Jun G, Beecham GW, Wang LS, Vardarajan BN, Buros J, Gallins PJ, Buxbaum JD, Jarvik GP, Crane PK *et al* (2011) Common variants at MS4A4/ MS4A6E, CD2AP, CD33 and EPHA1 are associated with late-onset Alzheimer's disease. *Nat Genet* 43: 436–441

Park JS, Burckhardt CJ, Lazcano R, Solis LM, Isogai T, Li L, Chen CS, Gao B, Minna JD, Bachoo R *et al* (2020) Mechanical regulation of glycolysis via cytoskeleton architecture. *Nature* 578: 621–626

Ponath G, Ramanan S, Mubarak M, Housley W, Lee S, Sahinkaya FR, Vortmeyer A, Raine CS, Pitt D (2017) Myelin phagocytosis by astrocytes after myelin damage promotes lesion pathology. *Brain* 140: 399–413

Qian Y, Yin J, Hong J, Li G, Zhang B, Liu G, Wan Q, Chen L (2016) Neuronal seipin knockout facilitates Aβ-induced neuroinflammation and neurotoxicity via reduction of PPARgamma in hippocampus of mouse. *J Neuroinflammation* 13: 145

Radde R, Bolmont T, Kaeser SA, Coomaraswamy J, Lindau D, Stoltze L, Calhoun ME, Jaggi F, Wolburg H, Gengler S *et al* (2006) Abeta42-driven cerebral amyloidosis in transgenic mice reveals early and robust pathology. *EMBO Rep* 7: 940–946

Raj T, Rothamel K, Mostafavi S, Ye C, Lee MN, Replogle JM, Feng T, Lee M, Asinovski N, Frohlich I *et al* (2014) Polarization of the effects of autoimmune and neurodegenerative risk alleles in leukocytes. *Science* 344: 519–523

Rey F, Balsari A, Giallongo T, Ottolenghi S, Di Giulio AM, Samaja M, Carelli S (2019) Erythropoietin as a neuroprotective molecule: an overview of its therapeutic potential in neurodegenerative diseases. *ASN Neuro* 11: 1759091419871420

Selkoe DJ, Hardy J (2016) The amyloid hypothesis of Alzheimer's disease at 25 years. *EMBO Mol Med* 8: 595–608

Semenza GL, Wang GL (1992) A nuclear factor induced by hypoxia via de novo protein synthesis binds to the human erythropoietin gene enhancer at a site required for transcriptional activation. *Mol Cell Biol* 12: 5447–5454

Shang YC, Chong ZZ, Wang S, Maiese K (2012) Prevention of beta-amyloid degeneration of microglia by erythropoietin depends on Wnt1, the PI 3-K/ mTOR pathway, bad, and Bcl-xL. *Aging (Albany NY)* 4: 187–201

Sole-Domenech S, Cruz DL, Capetillo-Zarate E, Maxfield FR (2016) The endocytic pathway in microglia during health, aging and Alzheimer's disease. *Ageing Res Rev* 32: 89–103

Sun J, Martin JM, Vanderpoel V, Sumbria RK (2019) The promises and challenges of erythropoietin for treatment of Alzheimer's disease. *Neuromolecular Med* 21: 12–24

Sun HL, Chen SH, Yu ZY, Cheng Y, Tian DY, Fan DY, He CY, Wang J, Sun PY, Chen Y *et al* (2020) Blood cell-produced amyloid-beta induces cerebral Alzheimer-type pathologies and behavioral deficits. *Mol Psychiatry* 26: 5568–5577

Tamaki C, Ohtsuki S, Iwatsubo T, Hashimoto T, Yamada K, Yabuki C, Terasaki T (2006) Major involvement of low-density lipoprotein receptor-related protein 1 in the clearance of plasma free amyloid beta-peptide by the liver. *Pharm Res* 23: 1407–1416

Tamura T, Aoyama M, Ukai S, Kakita H, Sobue K, Asai K (2017) Neuroprotective erythropoietin attenuates microglial activation, including morphological changes, phagocytosis, and cytokine production. *Brain Res* 1662: 65–74

Tansey KE, Cameron D, Hill MJ (2018) Genetic risk for Alzheimer's disease is concentrated in specific macrophage and microglial transcriptional networks. *Genome Med* 10: 14

Urena-Guerrero ME, Castaneda-Cabral JL, Rivera-Cervantes MC, Macias-Velez RJ, Jarero-Basulto JJ, Gudino-Cabrera G, Beas-Zarate C (2020)

Neuroprotective and neurorestorative effects of Epo and VEGF: perspectives for new therapeutic approaches to neurological diseases. *Curr Pharm Des* 26: 1263–1276

Wang C, Chen T, Li G, Zhou L, Sha S, Chen L (2015) Simvastatin prevents beta-amyloid(25-35)-impaired neurogenesis in hippocampal dentate gyrus through alpha7nAChR-dependent cascading PI3K-Akt and increasing BDNF via reduction of farnesyl pyrophosphate. *Neuropharmacology* 97: 122–132

Wang J, Gu BJ, Masters CL, Wang YJ (2017) A systemic view of Alzheimer disease - insights from amyloid-beta metabolism beyond the brain. *Nat Rev Neurol* 13: 612–623

Xiang Y, Bu XL, Liu YH, Zhu C, Shen LL, Jiao SS, Zhu XY, Giunta B, Tan J, Song WH *et al* (2015) Physiological amyloid-beta clearance in the periphery and

its therapeutic potential for Alzheimer's disease. *Acta Neuropathol* 130: 487–499

Xu L, Pan CL, Wu XH, Song JJ, Meng P, Li L, Wang L, Zhang Z, Zhang ZY (2021) Inhibition of Smad3 in macrophages promotes Aβ efflux from the brain and thereby ameliorates Alzheimer's pathology. *Brain Behav Immun* 95: 154–167

Zhi-Kun S, Hong-Qi Y, Zhi-Quan W, Jing P, Zhen H, Sheng-Di C (2012) Erythropoietin prevents PC12 cells from beta-amyloid-induced apoptosis via PI3KAkt pathway. *Transl Neurodegener* 1: 7

Zuroff L, Daley D, Black KL, Koronyo-Hamaoui M (2017) Clearance of cerebral Aβ in Alzheimer's disease: reassessing the role of microglia and monocytes. *Cell Mol Life Sci* 74: 2167–2201